Design and Analysis of FD MIMO Cellular System in coexistence with MIMO Radar

Design and Analysis of FD MIMO Cellular System in Coexistence with MIMO Radar

Sudip Biswas, Keshav Singh, Omid Taghizadeh, and Tharmalingam Ratnarajah

***Abstract*— Spectrum sharing and full duplexing are two promising technologies for alleviating the severe spectrum crunch that has threatened to blight the progress of future wireless communication systems. In this paper, we consider a two tier coexistence framework involving a collocated multiple-input-multiple-output (MIMO) radar system (RS) and a full-duplex MIMO cellular system (CS). Considering imperfect channel state information and hardware impairments at the CS, we focus on a spectrum sharing environment to improve the quality of service (QoS) for cellular users by designing i) precoders at CS via the minimization of sum mean-squared-errors, subject to the constraints of transmit powers of the CS and probability of detection (PoD) of the RS, and ii) precoders at the RS to mitigate the interference from RS towards CS. While the monotonically increasing relationship between PoD and its non-centrality parameter is exploited to resolve the PoD in terms of interference threshold towards the RS, a generalized likelihood ratio test for target detection is used to derive detector statistics of the precoded radar waveforms. Numerical results demonstrate the feasibility of the proposed spectrum sharing algorithms, albeit with certain tradeoffs in RS transmit power, PoD and QoS of cellular users.**

***Index Terms*—Multiple-input-multiple-output (MIMO), full-duplex (FD), spectrum sharing, MIMO radar, cellular system, precoder design, convex optimization.**

I. Introduction

Scant spectrum resources below 6 GHz and its highly inefficient utilization due to static spectrum allocation along with the exponentially increasing wireless data traffic are currently plaguing cellular network operators, which have heralded the emergence of research in i) spectrum sharing between commercial communication systems such as cellular systems and federal entities such as radars [1]–[3], and ii) full-duplex (FD) communications. As such, organisations around the world such as the Federal Communications Commission (FCC) is considering a number of options including incentive auctioning and sharing of federal spectrum to meet the commercial spectrum requirements. In particular, spectrum sharing is an attractive as well as a promising technology due to not only the availability of large number of underutilized federal spectrum bands, but also the fact that the high UHF radar bands overlap with GSM frequencies, and the S-band radar systems partially overlap with LTE and WiMAX systems. Nevertheless, spectrum sharing is associated with its inherent set of challenges because the incumbents need to be protected from the interference arising due to the operation of cellular systems in the shared bands. Further, it has not yet been possible for communication systems also to operate in the vicinity of radar systems on the same or adjacent frequency bands due to high transmit power of radars saturating communication system's receiver amplifiers.

With regards to FD, it can potentially double the spectrum efficiency of communication systems [4]–[7] by transmitting and receiving at the same time and frequency resources. However, this results in signal leakage from the transmitting antennas to its receiving antennas, also known as self-interference (SI), which dominates the performance of FD systems. Due to the recent advances in interference cancellation techniques [8], SI can be combated to the extent that only residual SI (RSI), which is caused due to the non-ideal nature of the transmit and receive hardware chains is left behind. This RSI can be mitigated through digital beamforming techniques, allowing us to truly explore the benefits of FD systems.

In light of the above, in this paper, we address the specific problem of cellular spectrum scarcity and propose a framework for improving the quality of service (QoS) of cellular users through efficient spectrum sharing between a multiple-input multiple-output (MIMO) radar and a cellular system equipped with a FD base station (BS). At this point, it is worth noting that most spectrum sharing approaches that are currently in practise are passive in nature as federal incumbents are not designed with sharing in mind, which places the entire burden on cellular systems to maintain an extremely high confidence level of interference protection towards federal entities by either transmitting in white spaces of the radar or not transmitting at all inside predefined exclusion zones that were recently introduced by National Telecommunications and Information Administration (NTIA). The potential for such conservative approaches is quite limited, which is reflected by their modest progress in becoming a business case for commercial deployment. In particular, while transmitting in white spaces only was not considered lucrative enough for cellular operators, it turned out that a large portion of the US population lives in the exclusion zones defined by NTIA. This issue is further highlighted in [9], which is illustrated through Fig. 1. The figure shows the percentage of spectrum that can be used as a function of the required confidence

Sudip Biswas is with the Department of Electronics and Communications Engineering, Indian Institute of Information Technology Guwahati, Guwahati 781015, India. He was previously with the Institute for Digital Communications, School of Engineering, University of Edinburgh, Edinburgh EH9 3JL, UK. (E-mail: sudip.biswas@iiitg.ac.in).

Keshav Singh is with the School of Electrical and Electronic Engineering, University College Dublin, Dublin 4, Ireland. (E-mail: keshav.singh@ucd.ie)

Omid Taghizadeh is with the Network Information Theory Group, Technische Universität Berlin, Berlin 10587, Germany. (E-mail: taghizadehmotlagh@tu-berlin.de)

T. Ratnarajah is with the Institute for Digital Communications, School of Engineering, University of Edinburgh, Edinburgh EH9 3JL, UK. (E-mail: tratnarajah@ed.ac.uk)

This work was supported by the UK Engineering and Physical Sciences Research Council (EPSRC) under grant no: EP/P009549/1 and the UK-India Education and Research Initiative Thematic Partnerships under grant no: DST-UKIERI-2016-17-0060.

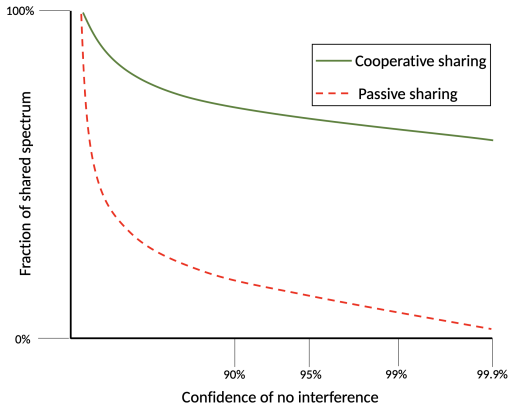

Fig. 1: Cooperative sharing vs passive sharing [9].

of 'no' or 'negligible' interference towards the incumbent. If the incumbent is originally designed with the anticipation of sharing and can cooperate with the cellular system, then a significantly higher fraction of idle spectrum can be utilized. The available spectrum can further be elevated by network operators by transmitting in FD mode, which will further increase the QoS and satisfaction ratio of the cellular users. Consequently, the next generation of spectrum sharing will focus not only on the design of the federal incumbents with the intention of sharing, but also the introduction of innovative technologies, such as FD at the communication system to make the most of the spectrum that is being made available through sharing.

Motivated by the above discussion, we consider a two-tier cooperative spectrum sharing model, where a MIMO radar system (RS) is the spectrum sharing entity and a FD MIMO cellular system (CS) is the beneficiary. With regards to existing literature, the contributions of this paper are summarized in the following:

- *Unlike [10]–[14], in this work we consider a framework wherein the CS BS, enabled with FD radio, serves multiple downlink (DL) and uplink (UL) users at the same time and frequency resources of the MIMO RS.* This is motivated by the idea of achieving higher spectral efficiency, where spectral coexistence is enabled simultaneously not only among the UL, DL users, but also the RS. In particular, we consider a system wherein the CS seeks to improve the users' QoS on the best-effort basis, while ensuring a guaranteed detection probability at the RS. *This is in contrast to prior works, e.g.,[16], [17], where the interference towards the RS is controlled on the best-effort basis, but subject to the hard requirements on the QoS at the CS.* Please note that the interference from the CS towards the RS is of utmost concern owing to the level of seriousness involved in the RS's operation.
- In order to concretize the treatment of the interference, both interference from the CS towards the RS as well as the interference towards the CS nodes and the tolerable detection probability at the RS as well as the communication performance at the CS are jointly considered under the impacts of hardware distortions [4], as well as the norm-bounded channel state information (CSI) error [7]. Furthermore, we consider a scenario where multi-antenna processing is enabled at the CS users, in addition to the MIMO FD BS. This improves the control of interference as it reduces the required transmit power for a given QoS in both UL and DL directions, while improving the beamforming capability at the UL. *This is in contrast to the prior works, which consider perfect hardware or CSI aquisition [14], [17], or consider single antenna users for the CS [11], [12], [17].*
- In order to maximize the QoS of the cellular users, linear precoder and equalizers are designed at the FD CS with the goal to minimize the Sum-MSE, for a given worst-case channel set, subject to the constraints of power budgets at the UL users and the FD BS, and detection probability performance at the MIMO RS. *Due to its good performance and low complexity, MSE-based transceiver design method [7], [18] is used in this paper. This is done by converting the resulting non-convex and semi-infinite optimization problem into a multi-convex semi-definite-programming (SDP) problem with a guaranteed convergence, where in each iteration a convex SDP subproblem is solved. On the radar side, precoders at the MIMO RS are designed in order to mitigate interference towards the FD CS. In particular, the interference channels from the RS towards the CS are used to calculate a null-space, which is then used to construct the precoding matrix based on the number of transmit antennas at the RS.*

Numerical simulations verify the effectiveness of the proposed approach, both in terms of the improved cellular performance as well as the maintained detection probability at the radar, under the consideration of practical parameter uncertainties. In comparison to the prior works, the current approach is far-reaching in the sense that it gives the cellular operators more confidence to utilize the spectrum of the radar, whereby it can focus more on its own users rather than the radar. Nevertheless, the radar is still protected, based on a pre-defined level of confidence (detection probability requirements) between the two entities.

Notations: Boldface capital and small letters denote matrices and vectors, respectively. The transpose, conjugate transpose and null space are respectively denoted by $(\cdot)^T$, $(\cdot)^H$, and $\mathcal{N}(\cdot)$. $\|\mathbf{A}\|_F$ and $\|\mathbf{a}\|_2$ denote the Frobenius norm of a matrix $\mathbf{A}$ and the Euclidean norm of a vector $\mathbf{a}$, respectively. The Kronecker tensor product is denoted by $\otimes$, while $\perp$ denotes the statistical independence. The matrices $\mathbf{I}_N$ and $\mathbf{O}_{M\times N}$ denote an $N \times N$ identity matrix and an $M \times N$ zero matrix, respectively. The notations $\mathbb{E}(\cdot)$ and $\mathrm{tr}(\cdot)$ refer to expectation and trace, respectively and $diag(\mathbf{A})$ generates a diagonal matrix with the same diagonal element as $\mathbf{A}$.

II. Spectrum Sharing Model and Preliminaries

We consider a cooperative spectrum sharing model, where a FD MU MIMO CS co-exists with a collocated MIMO RS over a bandwidth of B Hz as shown in Fig. 2. The CS comprises of a FD MIMO BS, equipped with M_0 transmit and N_0 receive antennas, that serves J DL and K UL users. Each DL and UL user is equipped with N_j receive and M_k transmit antennas, respectively and operates in HD mode. Further, the MIMO RS, which is located at the edge of the cell has R_T transmit

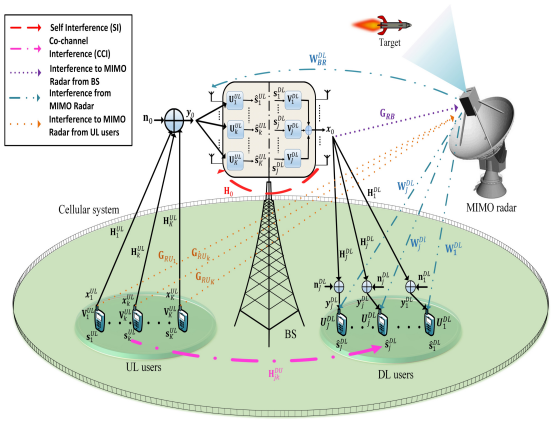

Fig. 2: A FD MU MIMO CS operating in the spectrum shared by a MIMO RS.

and R_R receive antennas for detecting/estimating a point-like target in the far-field.

1) Channel model: As shown in Fig. 2, $\mathbf{W}_i$ denote the interference channels shared by the MIMO RS with the CS, where $i = 1, \ldots, \mathcal{I}$, with $\mathcal{I} = 1 + J$, with $\mathbf{W}_{BR}^{DL} \in \mathbb{C}^{N_0 \times R_T}$ and $\mathbf{W}_j^{DL} \in \mathbb{C}^{N_j \times R_T}$ denoting the interference channels from RS's transmitter to BS and j-th DL user, respectively and $\mathbf{H}_k^{UL} \in \mathbb{C}^{N_0 \times M_k}$ and $\mathbf{H}_j^{DL} \in \mathbb{C}^{N_j \times M_0}$ represent the k-th UL and the j-th DL channel, respectively. The SI channel at the FD BS and the CCI channel between the k-th UL and j-th DL user are denoted as $\mathbf{H}_0 \in \mathbb{C}^{N_0 \times M_0}$ and $\mathbf{H}_{jk}^{DU} \in \mathbb{C}^{N_j \times M_k}$, respectively.

Let $\mathbf{s}_k^{UL} \in \mathbb{C}^{d_k^{UL} \times 1}$ and $\mathbf{s}_j^{DL} \in \mathbb{C}^{d_j^{DL} \times 1}$ denote the transmitted symbols by the k-th UL user and the FD BS, respectively, such that $\mathbb{E}\left[\mathbf{s}_k^{UL}\left(\mathbf{s}_k^{UL}\right)^H\right] = \mathbf{I}_{d_k^{UL}}$ and $\mathbb{E}\left[\mathbf{s}_j^{DL}\left(\mathbf{s}_j^{DL}\right)^H\right] = \mathbf{I}_{d_j^{DL}}$. The symbols $\mathbf{s}_k^{UL}$ and $\mathbf{s}_j^{DL}$ are first precoded by matrices $\mathbf{V}_k^{UL} \in \mathbb{C}^{M_k \times d_k^{UL}}$ and $\mathbf{V}_j^{DL} \in \mathbb{C}^{M_0 \times d_j^{DL}}$, respectively, such that the signals transmitted from the k-th UL user and the FD BS at time index l, with $l = 1, \ldots, L$ are given as $\mathbf{x}_k^{UL}(l) = \mathbf{V}_k^{UL}\mathbf{s}_k^{UL}(l)$ and $\mathbf{x}_0(l) = \sum_{j=1}^{J}\mathbf{V}_j^{DL}\mathbf{s}_j^{DL}(l)$, respectively. Here, L is total number of time samples for cellular communication. Similarly, the symbols $\mathbf{s}_R(l) \in \mathbb{C}^{R_T \times 1}$ transmitted by the RS at l-th time index, with $\mathbb{E}\left[\| \mathbf{s}_R(l) \|^2\right] \simeq \frac{1}{L_R}\sum_{l=1}^{L_R}\left[\mathbf{s}_R(l)\left(\mathbf{s}_R(l)\right)^H\right] = \mathbf{I}_{R_T}$ are first precoded by the matrix $\mathbf{P} \in \mathbb{C}^{R_T \times R_T}$ such that the transmitted signal becomes $\mathbf{x}_R = \mathbf{P}\mathbf{s}_R$. Here, L_R is the total number of time samples for the RS's communication. For the ease of derivation, hereinafter, we assume that the time duration of the RS's waveform is the same as the communication signals [19] with $L_R = L$. A list of the main notations are summarized in Table I on top of next page.

Now, considering hardware impairments at the FD BS and UL/DL users, the signals received at the CS utilizing the spectrum of MIMO RS can be written as

$$\begin{aligned}\mathbf{y}_0(l) =& \sum_{k=1}^{K}\mathbf{H}_k^{UL}\left(\mathbf{x}_k^{UL}(l) + \mathbf{c}_k^{UL}(l)\right) + \mathbf{H}_0\left(\mathbf{x}_0(l) + \mathbf{c}_0(l)\right) \\ &+\mathbf{e}_0(l) + \underbrace{\sqrt{P_R}\mathbf{W}_{BR}^{DL}\mathbf{x}_R(l)}_{\text{Interference from RS}} + \mathbf{n}_0(l), \end{aligned} \tag{1}$$

$$\begin{aligned}\mathbf{y}_j^{DL}(l) =& \mathbf{H}_j^{DL}\left(\mathbf{x}_0(l) + \mathbf{c}_0(l)\right) + \sum_{k=1}^{K}\mathbf{H}_{jk}^{DU}\left(\mathbf{x}_k^{UL}(l) + \mathbf{c}_k^{UL}(l)\right) \\ &+\mathbf{e}_j^{DL}(l) + \underbrace{\sqrt{P_R}\mathbf{W}_j^{DL}\mathbf{x}_R(l)}_{\text{Interference from RS}} + \mathbf{n}_j^{DL}(l), \end{aligned} \tag{2}$$

where $\mathbf{y}_0(l)$ and $\mathbf{y}_j^{DL}(l)$ are the signals received at FD BS and the j-th DL user at time index l and P_R denotes the RS's transmit power. The terms $\mathbf{n}_0(l) \in \mathbb{C}^{N_0}$ and $\mathbf{n}_j^{DL}(l) \in \mathbb{C}^{N_j}$ denote the additive white Gaussian noise (AWGN) vector with zero mean and covariance matrix $\mathbf{R}_0 = \sigma_0^2\mathbf{I}_{N_0}$ and $\mathbf{R}_j^{DL} = \sigma_j^2\mathbf{I}_{N_j}$ at the BS and the j-th DL user, respectively. Further, $\mathbf{c}_k^{UL}(l) \sim \mathcal{CN}\left(\mathbf{0}, \psi\,\mathrm{diag}\left(\mathbf{V}_k^{UL}\left(\mathbf{V}_k^{UL}\right)^H\right)\right)$, $\mathbf{c}_k^{UL}(l) \perp \mathbf{x}_k^{UL}(l)$ and $\mathbf{e}_j^{DL}(l) \sim \mathcal{CN}\left(\mathbf{0}, \upsilon\,\mathrm{diag}\left(\mathbf{\Phi}_j^{DL}\right)\right)$, $\mathbf{e}_j^{DL}(l) \perp \hat{\mathbf{u}}_j^{DL}(l)$ are the transmit and receive distortions[1] at the k-th UL user and the j-th DL user, respectively with $\psi \ll 1$ and $\upsilon \ll 1$. Here, $\mathbf{\Phi}_j^{DL} = \mathrm{Cov}\{\hat{\mathbf{u}}_j^{DL}(l)\}$ and $\hat{\mathbf{u}}_j^{DL}(l) = \mathbf{y}_j^{DL}(l) - \mathbf{e}_j^{DL}(l)$. The transmitter/receiver distortion model for $\mathbf{c}_0(l)$ and $\mathbf{e}_0(l)$ can also be defined in an equivalent way. Furthermore, the signal received by the MIMO RS at time index l from a single point target, in far-field with constant radial velocity $\tilde{v}_r$, at an angle θ can be written as

$$\begin{aligned}\mathbf{y}_R(l) =& \alpha_r\sqrt{P_R}e^{j\omega_D l}\mathbf{A}\left(\theta\right)\mathbf{x}_R(l - \tau(l)) \\ &+\mathbf{G}_{RB}\left(\sum_{j=1}^{J}\mathbf{V}_j^{DL}\mathbf{s}_j^{DL}(l) + \mathbf{c}_0(l)\right) \\ &+\sum_{k=1}^{K}\mathbf{G}_{RU_k}\left(\mathbf{V}_k^{UL}\mathbf{s}_k^{UL}(l) + \mathbf{c}_k^{UL}(l)\right) + \mathbf{n}_R(l), \end{aligned} \tag{3}$$

where $\tau(l) = \tau_t(l) + \tau_r(l)$ denotes the sum of propagation delays between the target and the t-th transmit element and the r-th receive element of the MIMO RS, respectively, while ω_D is the Doppler frequency shift. Here, $\mathbf{G}_{RB} \in \mathbb{C}^{R_R \times M_0}$ and $\mathbf{G}_{RU_k} \in \mathbb{C}^{R_R \times M_k}$ are the interference channels from BS and k-th UL user to the RS's receiver, respectively. Further, α_r indicates the complex path loss exponent of the radar-target-radar path including the propagation loss and the coefficient of reflection, $\mathbf{n}_R(l) \sim \mathcal{CN}\left(0, \sigma_R^2\mathbf{I}_R\right)$ and $\mathbf{A}\left(\theta\right)$ denotes the transmit-receive steering matrix and is expressed as

$$\mathbf{A}\left(\theta\right) \triangleq \mathbf{a}_R\left(\theta\right)\mathbf{a}_T^T\left(\theta\right). \tag{4}$$

In the above, $\mathbf{a}_T\left(\theta\right)$ is the transmit steering vector, defined as

$$\mathbf{a}_T\left(\theta\right) = \left[e^{-j\omega_c\tau_1(\theta)} \;\; e^{-j\omega_c\tau_2(\theta)} \;\; \ldots \;\; e^{-j\omega_c\tau_{R_T}(\theta)}\right]^T, \tag{5}$$

where ω_c is the carrier frequency. With assumptions $R_R = R_T = R$, we define $\mathbf{a}_R\left(\theta\right) = \mathbf{a}_T\left(\theta\right) = \mathbf{a}\left(\theta\right)$ and $\mathbf{A}_{ir}\left(\theta\right)$ as

$$\mathbf{A}_{ir}\left(\theta\right) = \exp\left(-j\frac{2\pi}{\lambda}\left[\sin\left(\theta\right); \cos\left(\theta\right)\right]^T\left(\mathbf{z}_i + \mathbf{z}_r\right)\right). \tag{6}$$

In particular, $\mathbf{A}_{ir}\left(\theta\right)$ denotes the i-th element at the r-th column of the matrix $\mathbf{A}$, $\mathbf{z}_i = \left[z_i^1; z_i^2\right]$ is the location of the i-th element of the antenna array and λ is the wavelength of the carrier.

To make the analysis tractable, hereinafter we consider the following assumptions:

- The path loss α is assumed to be identical for all transmit and receive elements, due to the far-field assumption.
- The angle θ is the azimuth angle of the target.
- After compensating the range-Doppler parameters, we can simplify (3) as

$$\begin{aligned}\mathbf{y}_R(l) =& \alpha_r\sqrt{P_R}\mathbf{A}\left(\theta\right)\mathbf{x}_R(l) + \mathbf{G}_{RB}\left(\sum_{j=1}^{J}\mathbf{V}_j^{DL}\mathbf{s}_j^{DL}(l) + \mathbf{c}_0(l)\right) \\ &+\sum_{k=1}^{K}\mathbf{G}_{RU_k}\left(\mathbf{V}_k^{UL}\mathbf{s}_k^{UL}(l) + \mathbf{c}_k^{UL}(l)\right) + \mathbf{n}_R(l). \end{aligned} \tag{7}$$

Remark 1: Note that Equations (1)- (7) indicate the observation of the cellular and radar signal at the specific time

[1]The imperfections in the transmitter/receiver chains (oscillators, analog-to-digital converters (ADCs), digital-to-analog converters (DACs), and power amplifiers), which resembles the RSI are modelled using the distortion model of [4].

TABLE I: Some important parameters and their definition

Parameter notation	Physical meaning
M_0/N_0	Number of transmit/receive antennas in the FD MIMO BS
J/K	Number of DL/UL users in the CS
N_j/N_0	Number of receive antennas at each DL/UL user
R_T/R_R	Number of transmit/receive antennas in MIMO RS
$\mathbf{W}_i$	Interference channels shared by the MIMO RS with the CS
$\mathbf{W}_{BR}^{DL}/\mathbf{W}_j^{DL}$	Interference channels from RS's transmitter to BS/j-th DL user
$\mathbf{H}_j^{DL}/\mathbf{H}_k^{UL}$	j-th DL/k-th UL channel
$\mathbf{H}_0/\mathbf{H}_{jk}$	SI channel/CCI channel
$\mathbf{G}_{RB}/\mathbf{G}_{RU_k}$	Interference channels from BS/k-th UL user to the RS's receiver
$\mathbf{V}_j^{DL}/\mathbf{V}_k^{UL}$	Precoding matrix at j-th DL/k-th UL user
$\sigma_R^2/\sigma_0^2/\sigma_j^2$	Noise power at the RS/BS/j-th DL user
$\mathbf{P}$	Precoding matrix at RS
P_R	RS's transmit power

instances, but does not imply symbol-level synchronization among the two systems. In fact, symbol-level synchronization is difficult to achieve due to the randomness of the radar function, as well as the lack of symbol-level collaboration. Accordingly, the subsequent derivations in this paper do not rely on symbol level synchronization and we abide by this notation for describing the signal model, for the sake of notational simplicity.

2) CSI acquisition: Acquiring CSI at both systems is important to ensure an interference free communication. Since cooperative sharing is considered in this paper, we assume that some amount of CSI, if not full is available at the communication nodes[2]. For the CS, providing its CSI to the RS is incentivized by the promise of zero interference from the RS. On the other hand, it is more challenging to obtain an accurate estimate of the CSI of the RS at the CS, as the RS might not be willing to cooperate with the CS owing to security concerns. Hence, it might not be possible to obtain a full CSI at the CS and only partial CSI may be obtained through techniques such as blind environmental learning [20], realization of a band manager with the authority of exchanging CSI between the RS and CS [21], etc. Hence, to model the imperfections caused due to imperfect CSI, in this paper we will consider a norm-bounded channel estimation error model for the links between the CS and RS.

Remark 2: Since the codeword $\mathbf{x}_0$ and the SI channel $\mathbf{H}_0$ are known by the CS's BS (due to the knowledge of its own transmitted signal), the term $\mathbf{H}_0\mathbf{x}_0$ in (1) can be cancelled out through SI mitigating techniques given in [7] and thus, the remaining part $\mathbf{H}_0\mathbf{c}_0$ can be treated as the RSI, which depends only on hardware imperfections. Nevertheless, the term $\mathbf{H}_0\mathbf{x}_0$ will be retained in the following sections for ease of understanding, but will be ignored in calculation of the numerical results.

III. Precoder Design at RS

Now that we know the interference terms involved in the considered spectrum sharing model, we can formulate the problems for both the systems to co-exist. In this section, we discuss the precoder design problem at the MIMO RS to mitigate the interference towards CS, while also deriving the necessary expressions for the statistical decision test for target detection.

[2]CSI estimation can be performed via the exchange of training sequences and feedback, and the application of usual CSI estimation methods [6].

A. Designing the precoder matrix $\mathbf{P}$

To enable spectrum sharing, the precoders are designed at the RS such that

$$\mathbf{W}_i\mathbf{P}\mathbf{s}_R = 0, \ \forall i \in \mathcal{I}. \tag{8}$$

The above criteria can be fulfilled if

$$\mathbf{P}\mathbf{s}_R \in \mathcal{N}(\mathbf{W}_i) \ \forall i \in \mathcal{I}, \tag{9}$$

which suggests that the projected RS signal $\mathbf{x}_R$ must lie in the null-space of the interference channels[3] $\mathbf{W}$. However, the validity of (8) and (9) is dependent on the number of antennas at the RS. Accordingly, in the following we consider two approaches for interference mitigation to enable spectrum sharing: a) full mitigation for $R_T \gg (N_0 + JN_j)$ and b) partial mitigation when $R_T \ll (N_0 + JN_j)$, but $R_T > N_0$ and $R_T > N_j$.

1) Full mitigation: Considering the availability of CSI of all the shared $\mathbf{W}$ channels at the RS, singular value decomposition (SVD) can be utilized to find $\mathbf{W}$, which can then be used to create the precoder matrix. The SVD of $\mathbf{W}$ can be given as

$$\mathbf{W} = \mathbf{R}\mathbf{\Omega}\mathbf{X}^H, \tag{10}$$

where $\mathbf{R}$ and $\mathbf{X}$ are unitary matrices and $\mathbf{\Omega}$ is a diagonal matrix whose elements are the singular values of $\mathbf{W}$. Now, let $\bar{\mathbf{\Omega}} \triangleq \text{diag}(\bar{\omega}_1 \dots \bar{\omega}_p)$, where $p \triangleq \min(N_0 + \sum_{j=1}^{J} N_j, R_T)$, $\bar{\omega}_1 > \bar{\omega}_2 > \dots \bar{\omega}_q = \bar{\omega}_{q+1} = \dots = \bar{\omega}_p = 0$ and $\tilde{\mathbf{\Omega}} \triangleq \text{diag}(\tilde{\omega}_1 \dots \tilde{\omega}_{R_T})$, where $\tilde{\omega}_r \triangleq 0, \forall r \leq q$, $\tilde{\omega}_r \triangleq 1, \forall r > q$, with $\bar{\mathbf{\Omega}}\tilde{\mathbf{\Omega}} = \mathbf{0}$. Using the above definitions, the precoder matrix can be defined as [15]

$$\mathbf{P} \triangleq \mathbf{X}\tilde{\mathbf{\Omega}}\mathbf{X}^H. \tag{11}$$

Remark 3: When additional information is available regarding the statistics of the target angles, or when the observation is of higher importance at a specific direction, the proposed null-space projection can be combined with a directional beamformer, emphasizing a set of target conditions over another.

Lemma 1: When $R_T \gg (N_0 + JN_j)$, the precoder matrix $\mathbf{P} \in \mathbb{C}^{R_T \times R_T}$ can be projected orthogonally onto $\mathbf{W}$, which encompasses the entire CS.

The above lemma holds due to the fact that $\mathbf{X}\mathbf{X}^H = \mathbf{I}$ as they are orthogonal matrices and $\tilde{\mathbf{\Omega}}^2 = \tilde{\mathbf{\Omega}}$ by construction. Further it can easily be shown that $\mathbf{P}\mathbf{x} - \mathbf{x} \in \mathcal{N}(\mathbf{P})$ for $\mathbf{x} \in \text{range}(\mathbf{P})$, which results in

$$\mathbf{W}\mathbf{P}^H = \mathbf{R}\bar{\mathbf{\Omega}}\mathbf{X}^H\mathbf{X}\tilde{\mathbf{\Omega}}\mathbf{X}^H = \mathbf{0}. \tag{12}$$

[3]Note that this assumption is not mandatory and is only considered to obtain a tractable theoretical framework.

2) Partial mitigation: If the MIMO RS has a smaller antenna array as compared to the combined antenna array of the FD BS and J downlink users, i.e. $R_T << (N_0 + JN_j)$, but is larger than individual antenna arrays of the CS, i.e. $R_T > N_0$ and $R_T > N_j$, then it is not possible for the MIMO RS to simultaneously mitigate interference towards the composite channel of all the DL users and the BS because of insufficient degrees of freedom. However, the available DoF can still be used to simultaneous detect a target and mitigate interference to either the BS or one of the users among the J users. The choice of user or BS selection depends upon the performance metric which radar wants to optimize. Prioritising the RS, we choose minimum degradation of radar waveform in a minimum norm sense as the performance metric. Hence, the problem now resorts to the selection of the interference channel which results in least degradation of the radar waveform and can be given as

$$\tilde{\mathbf{W}} = \{\mathbf{W}_i\}_{i_{min}}, \tag{13}$$

where

$$i_{min} \triangleq \underset{1\leq i\leq \mathcal{I}}{\operatorname{argmin}} \parallel \mathbf{P}_i \mathbf{s}_R(l) - \mathbf{s}_R(l) \parallel_2 . \tag{14}$$

Now, the precoder matrix can be defined as

$$\tilde{\mathbf{P}} \triangleq \mathbf{P}_{i_{min}} . \tag{15}$$

Remark 4: A drawback of partial mitigation scheme for spectrum sharing is that interference is mitigated to only one of the $J + 1$ DL nodes in the CS and the RS has to utilize higher transmit power to achieve the same performance level, which can increase the level of interference at the nodes not part of the mitigation scheme. This drawback can be addressed by $i)$ moving $(J + 1 - 1) = J$ nodes to non-radar frequency bands by using resource allocation and carrier aggregation techniques [22], $ii)$ modifying the MIMO RS's architecture as an overlapped-MIMO radar, where the transmit array of the colocated MIMO RS is partitioned into a number of subarrays that are allowed to overlap. The overlapped-MIMO RS architecture increases the DoF and enjoys the advantages of the MIMO radar while mitigating interference to communication systems without sacrificing the main desirable characteristics for its own transmission [23].

B. Target detection under spectrum sharing environment

Through a binary hypothesis test, we choose between two hypothesis for target detection and estimation. Using (7), the hypothesis testing problem can be written as

$$\mathbf{y}_R(l) = \begin{cases} \mathcal{H}_1 : \alpha_r \sqrt{P}_R \mathbf{A}(\theta) \mathbf{P} \mathbf{s}_R(l) \\ \quad + \mathbf{G}_{RB}\left(\sum_{j=1}^{J} \mathbf{V}_j^{DL} \mathbf{s}_j^{DL}(l) + \mathbf{c}_0\right) \\ \quad + \sum_{k=1}^{K} \mathbf{G}_{RU_k}\left(\mathbf{V}_k^{UL} \mathbf{s}_k^{UL}(l) + \mathbf{c}_k^{UL}\right) + \mathbf{n}_R(l), \\ \mathcal{H}_0 : \mathbf{G}_{RB}\left(\sum_{j=1}^{J} \mathbf{V}_j^{DL} \mathbf{s}_j^{DL}(l) + \mathbf{c}_0\right) \\ \quad + \sum_{k=1}^{K} \mathbf{G}_{RU_k}\left(\mathbf{V}_k^{UL} \mathbf{s}_k^{UL}(l) + \mathbf{c}_k^{UL}\right) + \mathbf{n}_R(l), \end{cases} \tag{16}$$

where $\mathcal{H}_0$ represents the case with no target but active CS and $\mathcal{H}_1$ indicates the case when the target and the CS are both active and $1 \leq l \leq L$. Since, the deterministic parameters α_r and θ are unknown, we adopt the generalized likelihood ratio test (GLRT) [24], which has the advantage of replacing the unknown parameters with their maximum likelihood (ML) estimates for determining the probability of detection (PoD). Hereinafter, by dropping the time index l for notational convenience (unless otherwise stated), the sufficient statistic of the received signal can be found using matched filtering as

$$\begin{aligned} \hat{\mathbf{Y}} = \frac{1}{\sqrt{L}} \sum_{l=1}^{L} \mathbf{y}_R \mathbf{x}_R^H = \alpha_r \sqrt{LP}_R \mathbf{A}(\theta) \mathbf{P}\mathbf{P}^H + \frac{1}{\sqrt{L}} \\ \times \sum_{l=1}^{L} \left(\mathbf{G}_{RB}\left(\sum_{j=1}^{J} \mathbf{V}_j^{DL} \mathbf{s}_j^{DL} + \mathbf{c}_0\right)\right. \\ \left. + \sum_{k=1}^{K} \mathbf{G}_{RU_k}\left(\mathbf{V}_k^{UL} \mathbf{s}_k^{UL} + \mathbf{c}_k^{UL}\right) + \mathbf{n}_R\right) \mathbf{s}_R^H \mathbf{P}^H. \end{aligned} \tag{17}$$

From (17), the vectorization of $\hat{\mathbf{Y}}$ can be written as

$$\begin{aligned} \hat{\mathbf{y}} =& \operatorname{vec}\left(\hat{\mathbf{Y}}\right) = \alpha_r \sqrt{LP}_R \operatorname{vec}\left(\mathbf{A}(\theta) \bar{\mathbf{P}}\right) \\ &+ \operatorname{vec}\left(\frac{1}{\sqrt{L}} \sum_{l=1}^{L} \left(\mathbf{G}_{RB}\left(\sum_{j=1}^{J} \mathbf{V}_j^{DL} \mathbf{s}_j^{DL} + \mathbf{c}_0\right)\right.\right. \\ &\left.\left. + \sum_{k=1}^{K} \mathbf{G}_{RU_k}\left(\mathbf{V}_k^{UL} \mathbf{s}_k^{UL} + \mathbf{c}_k^{UL}\right) + \mathbf{n}_R\right) \mathbf{P}^H \mathbf{s}_R^H\right) \\ &\triangleq \alpha_r \sqrt{LP}_R \operatorname{vec}\left(\mathbf{A}(\theta) \mathbf{P}^H\right) + \mathbf{\Psi}, \end{aligned} \tag{18}$$

where $\bar{\mathbf{P}} = \mathbf{P}\mathbf{P}^H = \mathbf{P}\mathbf{P} = \mathbf{P}$, $\bar{\mathbf{P}}\bar{\mathbf{P}}^H = \mathbf{P}\mathbf{P}^H\mathbf{P}\mathbf{P}^H = \mathbf{P}$ and $\mathbf{\Psi}$ is zero-mean, complex Gaussian distributed, and has a non-white block covariance matrix of

$$\boldsymbol{\chi} = \begin{pmatrix} \mathbf{P}^H(\tilde{\boldsymbol{\chi}} + \sigma_R^2 \mathbf{I}_R)\mathbf{P} & \cdots & \mathbf{0} \\ \vdots & \ddots & \vdots \\ \mathbf{0} & \cdots & \mathbf{P}^H(\tilde{\boldsymbol{\chi}} + \sigma_R^2 \mathbf{I}_R)\mathbf{P} \end{pmatrix}. \tag{19}$$

Here, $\boldsymbol{\chi} \in \mathbb{C}^{R^2 \times R^2}$ and $\tilde{\boldsymbol{\chi}} = \mathbf{G}_{RB} \sum_{j=1}^{J} \left(\mathbf{V}_j^{DL}\left(\mathbf{V}_j^{DL}\right)^H + \psi \operatorname{diag}\left(\mathbf{V}_j^{DL}\left(\mathbf{V}_j^{DL}\right)^H\right)\right)\left(\mathbf{G}_{RB}\right)^H + \sum_{k=1}^{K} \left(\mathbf{G}_{RU_k} \mathbf{V}_k^{UL}\left(\mathbf{V}_k^{UL}\right)^H \left(\mathbf{G}_{RU_k}\right)^H + \psi \operatorname{diag}\left(\mathbf{V}_k^{UL}\left(\mathbf{V}_k^{UL}\right)^H\right)\right)$.

However, the GLRT in [25] was applied in the presence of white noise only. Hence, to convert the covariance matrix in (19) into white, we apply a whitening filter $\mathbf{\Pi}^H$, obtained after the Cholesky decomposition[4] of $\boldsymbol{\chi}^{-1}$ as $\boldsymbol{\chi}^{-1} = \mathbf{\Pi}\mathbf{\Pi}^H$, with $\mathbf{\Pi}$ being a lower triangle matrix. Now, the hypothesis testing problem in (16) can be equivalently rewritten as

$$\hat{\mathbf{y}} = \begin{cases} \mathcal{H}_1 : \alpha_r \sqrt{LP}_R \mathbf{\Pi}^H \overline{\mathbf{A}}(\theta) + \mathbf{\Pi}^H \mathbf{\Psi}, \\ \mathcal{H}_0 : \mathbf{\Pi}^H \mathbf{\Psi}, \end{cases} \tag{20}$$

where $\overline{\mathbf{A}}(\theta) = \operatorname{vec}\left(\mathbf{A}(\theta) \bar{\mathbf{P}}\right)$. If $p\left(\hat{\mathbf{y}}, \hat{\alpha}_r, \hat{\theta}, \mathcal{H}_1\right)$ and $p(\hat{\mathbf{y}}, \mathcal{H}_0)$ denote the probability density function under $\mathcal{H}_1$ and $\mathcal{H}_0$, respectively, and $\hat{\alpha}_r$ and $\hat{\theta}$ indicate the ML estimation of α_r and θ under hypothesis $\mathcal{H}_1$, which is expressed as $\left[\hat{\alpha}_r, \hat{\theta}\right] = \max_{\alpha_r, \theta} p\left(\hat{\mathbf{y}} \mid \hat{\alpha}_r, \hat{\theta}, \mathcal{H}_1\right)$, then the GLRT can be given by

$$\begin{aligned} \ln L_{\hat{\mathbf{y}}}\left(\hat{\theta}_{ML}\right) =& \frac{\left|\overline{\mathbf{A}}^H\left(\hat{\theta}_{ML}\right) \mathbf{\Pi}\mathbf{\Pi}^H \hat{\mathbf{y}}\right|^2}{\left\|\mathbf{\Pi}^H \overline{\mathbf{A}}^H\left(\hat{\theta}_{ML}\right)\right\|^2} \lessgtr \bar{\delta}, \\ =& \frac{\left|\operatorname{tr}\left(\hat{\mathbf{Y}} \bar{\mathbf{P}}^H \mathbf{A}^H\left(\hat{\theta}_{ML}\right) \hat{\boldsymbol{\chi}}^{-1}\right)\right|^2}{\operatorname{tr}\left(\mathbf{A}\left(\hat{\theta}_{ML}\right) \bar{\mathbf{P}}\bar{\mathbf{P}}^H \mathbf{A}^H\left(\hat{\theta}_{ML}\right) \hat{\boldsymbol{\chi}}^{-1}\right)} \underset{\mathcal{H}_0}{\overset{\mathcal{H}_1}{\lessgtr}} \bar{\delta}, \end{aligned} \tag{21}$$

where $\bar{\delta}$ denotes the decision threshold and $\hat{\boldsymbol{\chi}} = \tilde{\boldsymbol{\chi}} + \sigma_R^2 \mathbf{I}_R$. According to [27], the asymptotic statistic of $L_{\hat{\mathbf{y}}}\left(\hat{\theta}_{ML}\right)$ for both the hypothesis is written as

$$\ln L_{\hat{\mathbf{y}}}\left(\hat{\theta}_{ML}\right) \backsim \begin{cases} \mathcal{H}_1 : \mathcal{X}_2^2(\rho), \\ \mathcal{H}_0 : \mathcal{X}_2^2, \end{cases} \tag{22}$$

where $\mathcal{X}_2^2$ denotes the central chi-squared distributions with two degrees of freedom (DoFs), $\mathcal{X}_2^2(\rho)$ is the non-central chi-squared distributions with two DoFs, and ρ indicates the non-central parameter given as

[4]Note that $\boldsymbol{\chi}$ and $\boldsymbol{\chi}^{-1}$ are both positive-definite Hermitian matrices.

$$\rho = \Gamma_R \sigma_R^2 \text{tr}\left(\mathbf{A}\left(\theta\right)\bar{\mathbf{P}}\bar{\mathbf{P}}^H\mathbf{A}^H\left(\theta\right)\hat{\boldsymbol{\chi}}^{-1}\right). \quad (23)$$

where $\Gamma_R = |\alpha_r|^2 LP_R/\sigma_R^2$. The decision threshold $\bar{\delta}$ is set according to a desired probability of false alarm P_{FA} as

$$\bar{\delta} = \mathfrak{F}^{-1}_{\mathcal{X}^2_2}\left(1 - P_{FA}\right), \quad (24)$$

where $\mathfrak{F}^{-1}_{\mathcal{X}^2_2}$ denotes the inverse central chi-squared distribution function with two DoFs. The PoD for the MIMO RS can now be given as

$$P_D = 1 - \mathfrak{F}_{\mathcal{X}^2_2(\rho)}\left(\mathfrak{F}^{-1}_{\mathcal{X}^2_2}\left(1 - P_{FA}\right)\right), \quad (25)$$

where $\mathfrak{F}_{\mathcal{X}^2_2(\rho)}$ is the non-central chi-squared distribution function with two DoFs.

IV. Precoder Design at CS

This section deals with the precoder design problem at the MIMO CS. The main goal of the CS is to provide the cellular users with service by utilizing the spectrum of the RS, but without affecting the PoD of RS [26]. We choose sum MSE as the performance metric for the CS, the rationale for which is that MSE-based optimization problems are equivalent to signal-to-interference-plus-noise ratio (SINR)-based optimization problems, since they are related as $\text{MSE} = 1/(1+\text{SINR})$. Hence, QoS based optimizations, which uses rate ($\log_2(1+\text{SINR})$) as cost functions can be conveniently transformed into MSE-based optimization as $-\log_2(\text{MSE})$. Accordingly, by applying linear receive filters $\mathbf{U}_k^{UL} \in \mathbb{C}^{N_0 \times d_k^{UL}}$ and $\mathbf{U}_j^{DL} \in \mathbb{C}^{N_j \times d_j^{DL}}$ to $\mathbf{y}_0$ and $\mathbf{y}_j^{DL}$ in (1)–(2), we obtain the source symbols of the k-th UL user at the BS and the j-th DL user, respectively as[5]

$$\hat{\mathbf{s}}_k^{UL} = \left(\mathbf{U}_k^{UL}\right)^H \left(\sum_{k=1}^{K}\mathbf{H}_k^{UL}\left(\mathbf{V}_k^{UL}\mathbf{s}_k^{UL} + \mathbf{c}_k^{UL}\right) + \mathbf{H}_0\left(\sum_{j=1}^{J}\mathbf{V}_j^{DL}\mathbf{s}_j^{DL} + \mathbf{c}_0\right) + \mathbf{e}_0 + \mathbf{W}_{BR}^{DL}\mathbf{x}_R + \mathbf{n}_0\right), \quad (26)$$

$$\hat{\mathbf{s}}_j^{DL} = \left(\mathbf{U}_j^{DL}\right)^H \left(\mathbf{H}_j^{DL}\left(\sum\nolimits_{j=1}^{J}\mathbf{V}_j^{DL}\mathbf{s}_j^{DL} + \mathbf{c}_0\right) + \sum\nolimits_{k=1}^{K}\mathbf{H}_{jk}^{DU}\left(\mathbf{V}_k^{UL}\mathbf{s}_k^{UL} + \mathbf{c}_k^{UL}\right) + \mathbf{e}_j^{DL} + \mathbf{W}_j^{DL}\mathbf{x}_R + \mathbf{n}_j^{DL}\right). \quad (27)$$

Lemma 2: The approximated aggregate interference-plus-noise terms at the k-th UL and j-th DL user, respectively, can be given respectively as[6]

$$\begin{aligned}\boldsymbol{\Pi}_k^{UL} \approx{}& \sum\nolimits_{j\neq k}^{K}\mathbf{H}_j^{UL}\mathbf{V}_j^{UL}\left(\mathbf{V}_j^{UL}\right)^H\left(\mathbf{H}_j^{UL}\right)^H + \psi\sum\nolimits_{j=1}^{K}\mathbf{H}_j^{UL}\text{diag}\left(\mathbf{V}_j^{UL}\left(\mathbf{V}_j^{UL}\right)^H\right)\left(\mathbf{H}_j^{UL}\right)^H \\ &+ \sum_{j=1}^{J}\mathbf{H}_0\left(\mathbf{V}_j^{DL}\left(\mathbf{V}_j^{DL}\right)^H + \psi\text{diag}\left(\mathbf{V}_j^{DL}\left(\mathbf{V}_j^{DL}\right)^H\right)\right)\mathbf{H}_0^H \\ &+ \upsilon\sum\nolimits_{j=1}^{J}\text{diag}\left(\mathbf{H}_0\mathbf{V}_j^{DL}\left(\mathbf{V}_j^{DL}\right)^H\mathbf{H}_0^H\right) + \upsilon\sum\nolimits_{j=1}^{K}\text{diag}\left(\mathbf{H}_j^{UL}\mathbf{V}_j^{UL}\left(\mathbf{V}_j^{UL}\right)^H\left(\mathbf{H}_j^{UL}\right)^H\right) \\ &+ P_R\left(\mathbf{W}_{BR}^{DL}\bar{\mathbf{P}}\left(\mathbf{W}_{BR}^{DL}\right)^H\right) + \sigma_0^2\mathbf{I}_{N_0}, \end{aligned} \quad (28)$$

$$\begin{aligned}\boldsymbol{\Pi}_j^{DL} \approx{}& \sum_{i\neq j}^{J}\mathbf{H}_j^{DL}\mathbf{V}_i^{DL}\left(\mathbf{V}_i^{DL}\right)^H\left(\mathbf{H}_j^{DL}\right)^H + \psi\sum_{i=1}^{J}\mathbf{H}_j^{DL}\text{diag}\left(\mathbf{V}_i^{DL}\left(\mathbf{V}_i^{DL}\right)^H\right)\left(\mathbf{H}_j^{DL}\right)^H \\ &+ \sum\nolimits_{k=1}^{K}\mathbf{H}_{jk}^{DU}\left(\mathbf{V}_k^{UL}\left(\mathbf{V}_k^{UL}\right)^H + \psi\text{diag}\left(\mathbf{V}_k^{UL}\left(\mathbf{V}_k^{UL}\right)^H\right)\right) \\ &\times\left(\mathbf{H}_{jk}^{DU}\right)^H + \upsilon\sum_{k=1}^{K}\text{diag}\left(\mathbf{H}_{jk}^{DU}\mathbf{V}_k^{UL}\left(\mathbf{V}_k^{UL}\right)^H\left(\mathbf{H}_{jk}^{DU}\right)^H\right) \\ &+ \upsilon\sum_{i=1}^{J}\text{diag}\left(\mathbf{H}_j^{DL}\mathbf{V}_i^{DL}\left(\mathbf{V}_i^{DL}\right)^H\left(\mathbf{H}_j^{DL}\right)^H\right) \\ &+ P_R\left(\mathbf{W}_j^{DL}\bar{\mathbf{P}}\left(\mathbf{W}_j^{DL}\right)^H\right) + \sigma_j^2\mathbf{I}_{N_j}. \end{aligned} \quad (29)$$

Proof: By considering $\psi << 1$ and $\upsilon << 1$ and ignoring the terms $\psi\upsilon$ and taking the expectation of the interference plus noise terms from (26) and (27), this lemma can be proved. ∎

Now, using estimates in (26) and (27) and Lemma 2, the MSEs of the k-th UL and j-th DL users can be written as

$$\begin{aligned}\mathbf{MSE}_k^{UL} = {}& \left(\left(\mathbf{U}_k^{UL}\right)^H\mathbf{H}_k^{UL}\mathbf{V}_k^{UL} - \mathbf{I}_{d_k^{UL}}\right) \\ &\times\left(\left(\mathbf{U}_k^{UL}\right)^H\mathbf{H}_k^{UL}\mathbf{V}_k^{UL} - \mathbf{I}_{d_k^{UL}}\right)^H + \left(\mathbf{U}_k^{UL}\right)^H\boldsymbol{\Pi}_k^{UL}\mathbf{U}_k^{UL}, \end{aligned} \quad (30)$$

$$\begin{aligned}\mathbf{MSE}_j^{DL} = {}& \left(\left(\mathbf{U}_j^{DL}\right)^H\mathbf{H}_j^{DL}\mathbf{V}_j^{DL} - \mathbf{I}_{d_j^{DL}}\right) \\ &\times\left(\left(\mathbf{U}_j^{DL}\right)^H\mathbf{H}_j^{DL}\mathbf{V}_j^{DL} - \mathbf{I}_{d_j^{DL}}\right)^H + \left(\mathbf{U}_j^{DL}\right)^H\boldsymbol{\Pi}_j^{DL}\mathbf{U}_j^{DL}, \end{aligned} \quad (31)$$

which will now be used to formulate the beamforming design problem at the CS.

1) Sum-MSE Minimization Problem Formulation: The joint problem can be formulated as

$$\begin{aligned}\textbf{(P0)}\ \min_{\mathbf{V},\mathbf{U}}\ & \sum_{k=1}^{K}\text{tr}\left\{\mathbf{MSE}_k^{UL}\right\} + \sum_{j=1}^{J}\text{tr}\left\{\mathbf{MSE}_j^{DL}\right\}, \quad (32)\\ \text{s.t}\quad & (C.1)\quad \text{tr}\left\{\mathbf{V}_k^{UL}\left(\mathbf{V}_k^{UL}\right)^H\right\} \le P_k,\ k = 1,\ldots,K, \\ & (C.2)\quad \sum\nolimits_{j=1}^{J}\text{tr}\left\{\mathbf{V}_j^{DL}\left(\mathbf{V}_j^{DL}\right)^H\right\} \le P_0, \\ & (C.3)\quad P_D \ge \Theta,\ \Theta \in (0,1]. \end{aligned}$$

In the above P_k is the transmit power constraint at the k-th UL user, P_0 is the total power constraint at the BS, and Θ is the threshold for PoD set by the MIMO RS. The sets of all transmit and receive beamforming matrices are denoted by $\mathbf{V} = \left\{\mathbf{V}_k^{UL},\ \mathbf{V}_j^{DL}\right\}$ and $\mathbf{U} = \left\{\mathbf{U}_k^{UL},\ \mathbf{U}_j^{DL}\right\}$, respectively. Note that P_D is a monotonically increasing function with respect to the non-central parameter (ρ in this case) [27]. Hence, we can equivalently reformulate the problem **(P0)** as

$$\begin{aligned}\textbf{(P1)}\quad \min_{\mathbf{V},\mathbf{U}}\ & \sum_{k=1}^{K}\text{tr}\left\{\mathbf{MSE}_k^{UL}\right\} + \sum_{j=1}^{J}\text{tr}\left\{\mathbf{MSE}_j^{DL}\right\}, \quad (33)\\ \text{s.t}\quad & (C.1)\quad \text{tr}\left\{\mathbf{V}_k^{UL}\left(\mathbf{V}_k^{UL}\right)^H\right\} \le P_k,\ k = 1,\ldots,K, \\ & (C.2)\quad \sum\nolimits_{j=1}^{J}\text{tr}\left\{\mathbf{V}_j^{DL}\left(\mathbf{V}_j^{DL}\right)^H\right\} \le P_0, \\ & (C.3)\quad \text{tr}\left(\mathbf{A}\left(\theta\right)\ \bar{\mathbf{P}}\bar{\mathbf{P}}^H\mathbf{A}^H\left(\theta\right)\hat{\boldsymbol{\chi}}^{-1}\right) \ge \Theta,\ \Theta \in (0,1]. \end{aligned}$$

[5]The terms $\mathbf{W}_{BR}^{DL}\mathbf{x}_R$ and $\mathbf{W}_j^{DL}\mathbf{x}_R$ are removed by the RS through precoder design as shown in Section III. However, they are kept in the mathematical analysis in this section for tractability. Nevertheless, they will not been considered in the numerical results.

[6]Note that approximation of $\boldsymbol{\Pi}_k^{UL}$ and $\boldsymbol{\Pi}_j^{DL}$ is a practical assumption [4]. The values of ψ and υ are much lower than 1. However, their values might not be negligible under a strong SI channel.

However, the constraint $(C.2)$ in **(P1)** is non-convex [28], and the problem cannot be solved in its current form. Hence, for tractability a lower bound on $(C.2)$ is considered.

Lemma 3: Let $\varphi = \text{tr}(\bar{\mathbf{P}}\bar{\mathbf{P}}^H)$. For $R_T = R_R = R$, a lower bound for $\text{tr}\left(\mathbf{A}(\theta)\bar{\mathbf{P}}\bar{\mathbf{P}}^H\mathbf{A}^H(\theta)\hat{\boldsymbol{\chi}}^{-1}\right)$ can be given as

$$\text{tr}\left(\mathbf{A}(\theta)\bar{\mathbf{P}}\bar{\mathbf{P}}^H\mathbf{A}^H(\theta)\hat{\boldsymbol{\chi}}^{-1}\right) \geq \frac{\varphi R^2}{I^{RAD}+R\sigma_R^2}, \tag{34}$$

where I^{RAD} is the total interference power from the CS to the MIMO RS and is given as

$$\begin{aligned} I^{RAD} = &\sum\nolimits_{k=1}^{K} \text{tr}\Big\{\mathbf{G}_{RU_k}\Big(\mathbf{V}_k^{UL}\left(\mathbf{V}_k^{UL}\right)^H \\ &+\psi\text{diag}\left(\mathbf{V}_k^{UL}\left(\mathbf{V}_k^{UL}\right)^H\right)\Big)(\mathbf{G}_{RU_k})^H\Big\} \\ &+\sum\nolimits_{j=1}^{J}\text{tr}\Big\{\mathbf{G}_{RB}\Big(\mathbf{V}_j^{DL}\left(\mathbf{V}_j^{DL}\right)^H \\ &+\psi\text{diag}\left(\mathbf{V}_j^{DL}\left(\mathbf{V}_j^{DL}\right)^H\right)\Big)(\mathbf{G}_{RB})^H\Big\}. \end{aligned} \tag{35}$$

Proof: The proof is given in Appendix B. ∎

Applying Lemma 3, the problem **(P1)** can be equivalently transformed as

$$\begin{aligned} \textbf{(P1.A)}\ &\min_{\mathbf{V},\mathbf{U}} \sum\nolimits_{k=1}^{K}\text{tr}\left\{\mathbf{MSE}_k^{UL}\right\}+\sum\nolimits_{j=1}^{J}\text{tr}\left\{\mathbf{MSE}_j^{DL}\right\}, \quad (36)\\ \text{s.t}\quad &(C.1)\quad \text{tr}\left\{\mathbf{V}_k^{UL}\left(\mathbf{V}_k^{UL}\right)^H\right\}\leq P_k,\ k=1,\ldots,K,\\ &(C.2)\quad \sum\nolimits_{j=1}^{J}\text{tr}\left\{\mathbf{V}_j^{DL}\left(\mathbf{V}_j^{DL}\right)^H\right\}\leq P_0,\\ &(C.3)\quad I^{RAD}\leq\Gamma(\Theta), \end{aligned}$$

where $\Gamma(\Theta)$ is the interference temperature threshold set by the RS and is intrinsically related to P_D. However, for simplicity, henceforth, we will denote $\Gamma(\Theta)$ with Γ.

Hereinafter, similar to [5], [29], we simplify the notations by combining UL and DL channels. Suppose that the symbols $\mathcal{S}^{UL}$ and $\mathcal{S}^{DL}$ denote the set of K UL and J DL channels, respectively, while the channels from radar to BS and the set of J DL channels from radar to DL users are expressed by $\mathcal{S}_{BU}^{DL}$ and $\mathcal{S}_{BR}^{DL}$, respectively. Denoting $\mathbf{V}_i^X$, $\mathbf{U}_i^X$, d_i^X and $\mathbf{\Pi}_i^X$, $X\in\{UL,DL\}$ as $\mathbf{V}_i$, $\mathbf{U}_i$, d_i and $\mathbf{\Pi}_i$, respectively, and expressing $\mathbf{H}_{ij}$, $\mathbf{G}_{R_j}$, $\mathbf{n}_i$, and receive (transmit) antenna numbers $\tilde{N}_i\left(\tilde{M}_i\right)$ as shown in Table II on top of next page. Using simplified notations, the i-th link MSE, $i\in\mathcal{S}\triangleq\mathcal{S}^{UL}\cup\mathcal{S}^{DL}$ is expressed as

$$\mathbf{MSE}_i=\left(\mathbf{U}_i^H\mathbf{H}_{ii}\mathbf{V}_i-\mathbf{I}_{d_i}\right)\left(\mathbf{U}_i^H\mathbf{H}_{ii}\mathbf{V}_i-\mathbf{I}_{d_i}\right)^H+\mathbf{U}_i^H\mathbf{\Pi}_i\mathbf{U}_i, \tag{37}$$

where

$$\begin{aligned} \mathbf{\Pi}_i=&\sum_{j\in\mathcal{S},j\neq i}\mathbf{H}_{ij}\mathbf{V}_j\mathbf{V}_j^H\mathbf{H}_{ij}^H+\psi\sum\nolimits_{j\in\mathcal{S}}\mathbf{H}_{ij}\text{diag}\left(\mathbf{V}_j\mathbf{V}_j^H\right)\mathbf{H}_{ij}^H\\ &+\upsilon\sum\nolimits_{j\in\mathcal{S}}\text{diag}\left(\mathbf{H}_{ij}\mathbf{V}_j\mathbf{V}_j^H\mathbf{H}_{ij}^H\right)+P_R\left(\mathbf{W}_i\bar{\mathbf{P}}(\mathbf{W}_i)^H\right)+\sigma_i^2\mathbf{I}_{\tilde{N}_i} \end{aligned} \tag{38}$$

and I^{RAD} in (35) is expressed as

$$I^{RAD}=\sum\nolimits_{j\in\mathcal{S}}\text{tr}\left\{\mathbf{G}_{R_j}\left(\mathbf{V}_j\mathbf{V}_j^H+\psi\text{diag}\left(\mathbf{V}_j\mathbf{V}_j^H\right)\right)\mathbf{G}_{R_j}^H\right\}. \tag{39}$$

2) Robust Design: In order to design a more practical and robust system, we assume that the FD BS does not have perfect CSI knowledge of the cellular users and RS. By considering the worst-case (norm-bounded error) model [30], the channel uncertainties can be defined as

$$\mathbf{H}_{ij}\in\mathcal{H}_{ij} = \left\{\tilde{\mathbf{H}}_{ij}+\boldsymbol{\Delta_i}:\|\boldsymbol{\Delta_i}\|_F\leq\delta_i,\ j\in\mathcal{S}\right\}, \tag{40}$$

$$\mathbf{G}_{R_j}\in\mathcal{G}_j = \left\{\tilde{\mathbf{G}}_{R_j}+\mathbf{\Lambda}:\|\mathbf{\Lambda}\|_F\leq\hat{\varrho},\ j\in\mathcal{S}\right\}, \tag{41}$$

where $\{\tilde{\mathbf{H}}_{ij}\}$ and $\{\tilde{\mathbf{G}}_j\}$ are the estimated CSI, while $\{\boldsymbol{\Delta_i}\}$ and $\mathbf{\Lambda}$ are the CSI error matrix. The symbols $\{\delta_i\}$ and $\hat{\varrho}$ are used to express the uncertainty bounds.

Using (37), (40) and (41) and the simplified notations, the optimization problem **(P1.A)** can be reformulated as a robust optimization problem as

$$\begin{aligned} \textbf{(P2)}\quad &\min_{\mathbf{V},\mathbf{U}}\ \max_{\forall\mathbf{H}_{ij}\in\mathcal{H}_{ij}}\sum\nolimits_{i\in\mathcal{S}}\text{tr}\{\mathbf{MSE}_i\} \quad (42)\\ \text{s.t}\quad &(C.1)\quad \text{tr}\left\{\mathbf{V}_i\mathbf{V}_i^H\right\}\leq P_i,\ i\in\mathcal{S}^{UL},\\ &(C.2)\quad \sum\nolimits_{i\in\mathcal{S}^{DL}}\text{tr}\left\{\mathbf{V}_i\mathbf{V}_i^H\right\}\leq P_0,\\ &(C.3)\quad I^{RAD}\leq\Gamma,\ \forall\mathbf{G}_{R_j}\in\mathcal{G}_j. \end{aligned}$$

The problem **(P2)** is a semi-infinite problem [31, Ch. 3] because of the constraint $C.3$ in (42), and thus is intractable. To make it tractable, we transform the problem **(P2)** into an equivalent SDP problem by converting the constraints into equivalent linear matrix inequality (LMI) forms. By using epigraph method [28] and introducing slack variables $\boldsymbol{\tau}=\{\tau_i\},\ i\in\mathcal{S}$, we reformulate the min-max problem **(P2)** as a minimization problem as

$$\begin{aligned} \textbf{(P3)}\quad &\min_{\mathbf{V},\mathbf{U},\boldsymbol{\tau}}\ \sum\nolimits_{i\in\mathcal{S}}\tau_i \quad (43)\\ \text{s.t}\quad &(C.1)\quad \text{tr}\{\mathbf{MSE}_i\}\leq\tau_i,\ \forall\mathbf{H}_{ij}\in\mathcal{H}_{ij},\ i\in\mathcal{S},\\ &(C.2)\quad \text{tr}\left\{\mathbf{V}_i\mathbf{V}_i^H\right\}\leq P_i,\ i\in\mathcal{S}^{UL},\\ &(C.3)\quad \sum\nolimits_{i\in\mathcal{S}^{DL}}\text{tr}\left\{\mathbf{V}_i\mathbf{V}_i^H\right\}\leq P_0,\\ &(C.4)\quad I^{RAD}\leq\Gamma,\ \forall\mathbf{G}_{R_j}\in\mathcal{G}_j. \end{aligned}$$

The objective function in **(P3)** is linear and thus problem **(P3)** can be reformulated as a standard SDP problem with LMI constraints. However, before solving the problem **(P3)**, we need to write $\text{tr}\{\mathbf{MSE}_i\}$ and I^{RAD} into vector forms and relax the semi-infinite constraints $(C.1)$ of **(P3)** and $(C.3)$ of **(P2)** with bounded norms.

Lemma 4: The vector forms of $\text{tr}\{\mathbf{MSE}_i\}$ and I^{RAD} can be written as $\text{tr}\{\mathbf{MSE}_i\}=\|\boldsymbol{\mu}_i\|_2^2$ and $I^{RAD}=\|\boldsymbol{\iota}\|_2^2$, where $\boldsymbol{\mu}_i$ and $\boldsymbol{\iota}$ are given as[7]

$$\boldsymbol{\mu}_i=\begin{bmatrix}\left(\mathbf{V}_i^T\otimes\mathbf{U}_i^H\right)\text{vec}\left(\mathbf{H}_{ii}\right)-\text{vec}\left(\mathbf{I}_{d_i}\right)\\ \left\lfloor\left(\mathbf{V}_j^T\otimes\mathbf{U}_i^H\right)\text{vec}\left(\mathbf{H}_{ij}\right)\right\rfloor_{j\in\mathcal{S},j\neq i}\\ \left\lfloor\left\lfloor\sqrt{\psi}\left((\mathbf{\Xi}_\ell\mathbf{V}_j)^T\otimes\mathbf{U}_i^H\right)\text{vec}\left(\mathbf{H}_{ij}\right)\right\rfloor_{\ell\in\mathcal{D}_j^{(\tilde{M})}}\right\rfloor_{j\in\mathcal{S}}\\ \left\lfloor\left\lfloor\sqrt{\upsilon}\left(\mathbf{V}_j^T\otimes(\mathbf{U}_i^H\mathbf{\Xi}_\ell)\right)\text{vec}\left(\mathbf{H}_{ij}\right)\right\rfloor_{\ell\in\mathcal{D}_i^{(\tilde{N})}}\right\rfloor_{j\in\mathcal{S}}\\ P_R\left(\mathbf{I}_R^T\otimes\mathbf{U}_i^H\right)\text{vec}\left(\mathbf{W}_i\bar{\mathbf{P}}\right)\\ \sigma_i\text{vec}\left(\mathbf{U}_i\right)\end{bmatrix}, \tag{44}$$

$$\boldsymbol{\iota}=\begin{bmatrix}\left\lfloor\left(\mathbf{V}_j^T\otimes\mathbf{I}_R\right)\text{vec}\left(\mathbf{G}_j\right)\right\rfloor_{j\in\mathcal{S}}\\ \sqrt{\psi}\left\lfloor\left\lfloor\left((\mathbf{\Xi}_\ell\mathbf{V}_j)^T\otimes\mathbf{I}_R\right)\text{vec}\left(\mathbf{G}_j\right)\right\rfloor_{\ell\in\mathcal{D}_j^{(\tilde{M})}}\right\rfloor_{j\in\mathcal{S}}\end{bmatrix}, \tag{45}$$

[7]For the sake of simplicity, we assume $\tilde{M}=M_0=M_i,\ i\in\mathcal{S}^{UL}$.

TABLE II: Simplified Notations

$\mathbf{H}_{ij}$	$\mathbf{H}_j^{UL}, i \in \mathcal{S}^{UL},\ j \in \mathcal{S}^{UL};\ \mathbf{H}_0, i \in \mathcal{S}^{UL},\ j \in \mathcal{S}^{DL}; \mathbf{H}_{ij}^{DU}, i \in \mathcal{S}^{DL},\ j \in \mathcal{S}^{UL}; \mathbf{H}_i^{DL}, i \in \mathcal{S}^{DL},\ j \in \mathcal{S}^{DL}$
$\mathbf{G}_{R_j}$	$\mathbf{G}_{RU_j}, j \in \mathcal{S}^{UL}; \mathbf{G}_{RB}, j \in \mathcal{S}^{DL}$
$\mathbf{W}_i$	$\mathbf{W}_i^{DL}, i \in \mathcal{S}^{DL}; \mathbf{W}_{BR}^{DL}, i \in \mathcal{S}_{BR}^{DL}$
$\mathbf{n}_i$	$\mathbf{n}_0, i \in \mathcal{S}^{UL}; \mathbf{n}_i^{DL}, i \in \mathcal{S}^{DL}$
$\tilde{N}_i(\tilde{M}_i)$	$N_0(M_i), i \in \mathcal{S}^{UL}; N_i(M_0), i \in \mathcal{S}^{DL}$

where $\mathbf{\Xi}_\ell$ denotes a square matrix with zero as elements, except for the ℓ-th diagonal element, which is equal to 1. $\mathcal{D}_j^{(\tilde{N})}$ and $\mathcal{D}_j^{(\tilde{M})}$ indicate the set $\{1 \cdots \tilde{N}_j\}$ and $\{1 \cdots \tilde{M}_j\}$, respectively.

Proof: The proof is given in Appendix C. ∎

Proposition 1: Using the vector forms in Lemma (4), the semi-infinite problem **(P3)** can be equivalently reformulated as a SDP problem as

$$\textbf{(P4)} \quad \min_{\mathbf{V},\mathbf{U},\boldsymbol{\tau},\epsilon_i \geq 0, \eta \geq 0} \sum\nolimits_{i \in \mathcal{S}} \tau_i \tag{46}$$

$$\text{s.t } (C.1) \quad \begin{bmatrix} \tau_i - \epsilon_i & \tilde{\boldsymbol{\mu}}_i^H & \mathbf{0}_{1 \times \tilde{N}_i \tilde{M}} \\ \tilde{\boldsymbol{\mu}}_i & \mathbf{I}_{A_i} & -\delta_i \mathbf{D}_{\Delta_i} \\ \mathbf{0}_{\tilde{N}_i \tilde{M} \times 1} & -\delta_i \mathbf{D}_{\Delta_i}^H & \epsilon_i \mathbf{I}_{\tilde{N}_i \tilde{M}} \end{bmatrix} \succeq 0,\ i \in \mathcal{S},$$

$$(C.2) \quad \|\mathrm{vec}(\mathbf{V}_i)\|_2^2 \leq P_i,\ i \in \mathcal{S}^{UL},$$

$$(C.3) \quad \|\lfloor \mathrm{vec}(\mathbf{V}_i) \rfloor_{i \in \mathcal{S}^{DL}}\|_2^2 \leq P_0,$$

$$(C.4) \quad \begin{bmatrix} \Gamma - \eta & \tilde{\boldsymbol{\iota}}^H & \mathbf{0}_{1 \times R\tilde{M}} \\ \tilde{\boldsymbol{\iota}} & \mathbf{I}_B & -\hat{\varrho} \mathbf{E}_\Lambda \\ \mathbf{0}_{R\tilde{M} \times 1} & -\hat{\varrho} \mathbf{E}_\Lambda^H & \eta \mathbf{I}_{R\tilde{M}} \end{bmatrix} \succeq 0.$$

The terms A_i, B, $\tilde{\boldsymbol{\mu}}_i$, $\mathbf{D}_{\Delta_i}$, $\tilde{\boldsymbol{\iota}}$, and $\mathbf{E}_\Lambda$ in **(P4)** are explicitly defined as

$$A_i = d_i \left(\sum\nolimits_{j \in \mathcal{S}} \left(d_j + \tilde{M}_j \right) + \tilde{N}_i \right) + \tilde{N}_i \sum\nolimits_{j \in \mathcal{S}} d_j, \tag{47}$$

$$B = R \sum\nolimits_{j \in \mathcal{S}} \left(d_j + \tilde{M}_j \right), \tag{48}$$

$$\tilde{\boldsymbol{\mu}}_i = \begin{bmatrix} \left(\mathbf{V}_i^T \otimes \mathbf{U}_i^H\right) \mathrm{vec}\left(\tilde{\mathbf{H}}_{ii}\right) - \mathrm{vec}\left(\mathbf{I}_{d_i}\right) \\ \left\lfloor \left(\mathbf{V}_j^T \otimes \mathbf{U}_i^H\right) \mathrm{vec}\left(\tilde{\mathbf{H}}_{ij}\right) \right\rfloor_{j \in \mathcal{S}, j \neq i} \\ \left[\left\lfloor \sqrt{\psi} \left((\mathbf{\Xi}_\ell \mathbf{V}_j)^T \otimes \mathbf{U}_i^H \right) \mathrm{vec}\left(\tilde{\mathbf{H}}_{ij}\right) \right\rfloor_{\ell \in \mathcal{D}_j^{(\tilde{M})}} \right]_{j \in \mathcal{S}} \\ \left[\left\lfloor \sqrt{\upsilon} \left(\mathbf{V}_j^T \otimes (\mathbf{U}_i^H \mathbf{\Xi}_\ell) \right) \mathrm{vec}\left(\tilde{\mathbf{H}}_{ij}\right) \right\rfloor_{\ell \in \mathcal{D}_i^{(\tilde{N})}} \right]_{j \in \mathcal{S}} \\ P_R \left(\mathbf{I}_R \otimes \mathbf{U}_i^H\right) \mathrm{vec}\left(\mathbf{W}_i \bar{\mathbf{P}}\right) \\ \sigma_i \mathrm{vec}\left(\mathbf{U}_i\right) \end{bmatrix}, \tag{49}$$

$$\mathbf{D}_{\Delta_i} = \underbrace{\begin{bmatrix} \left(\mathbf{V}_i^T \otimes \mathbf{U}_i^H\right) \\ \left\lfloor \left(\mathbf{V}_j^T \otimes \mathbf{U}_i^H\right) \right\rfloor_{j \in \mathcal{S}, j \neq i} \\ \left[\left\lfloor \sqrt{\psi} \left((\mathbf{\Xi}_\ell \mathbf{V}_j)^T \otimes \mathbf{U}_i^H \right) \right\rfloor_{\ell \in \mathcal{D}_j^{(\tilde{M})}} \right]_{j \in \mathcal{S}} \\ \left[\left\lfloor \sqrt{\upsilon} \left(\mathbf{V}_j^T \otimes (\mathbf{U}_i^H \mathbf{\Xi}_\ell) \right) \right\rfloor_{\ell \in \mathcal{D}_i^{(\tilde{N})}} \right]_{j \in \mathcal{S}} \\ \mathbf{0}_{d_i \tilde{N}_i \times \tilde{N}_i \tilde{M}} \\ \mathbf{0}_{d_i \tilde{N}_i \times \tilde{N}_i \tilde{M}} \end{bmatrix}}_{\mathbf{D}_{\Delta_i}} \mathrm{vec}\left(\boldsymbol{\Delta}_i\right), \tag{50}$$

$$\tilde{\boldsymbol{\iota}} = \begin{bmatrix} \left\lfloor \left(\mathbf{V}_j^T \otimes \mathbf{I}_R\right) \mathrm{vec}\left(\tilde{\mathbf{G}}_{lj}\right) \right\rfloor_{j \in \mathcal{S}} \\ \sqrt{\psi} \left[\left\lfloor \left((\mathbf{\Xi}_\ell \mathbf{V}_j)^T \otimes \mathbf{I}_R \right) \mathrm{vec}\left(\tilde{\mathbf{G}}_{lj}\right) \right\rfloor_{\ell \in \mathcal{D}_j^{(\tilde{M})}} \right]_{j \in \mathcal{S}} \end{bmatrix}, \tag{51}$$

$$\mathbf{E}_\Lambda = \underbrace{\begin{bmatrix} \left\lfloor \left(\mathbf{V}_j^T \otimes \mathbf{I}_R\right) \right\rfloor_{j \in \mathcal{S}} \\ \sqrt{\psi} \left[\left\lfloor \left((\mathbf{\Xi}_\ell \mathbf{V}_j)^T \otimes \mathbf{I}_R \right) \right\rfloor_{\ell \in \mathcal{D}_j^{(\tilde{M})}} \right]_{j \in \mathcal{S}} \end{bmatrix}}_{\mathbf{E}_\Lambda} \mathrm{vec}\left(\mathbf{\Lambda}\right). \tag{52}$$

Proof: The proof is given in Appendix D. ∎

Note that the problem **(P4)** is not jointly convex over variables $\mathbf{V}$ and $\mathbf{U}$. However, it is separately convex over each of the variables. Therefore, an alternating optimization method is adopted to solve the problem. This alternating minimization process is continued until a stationary point is reached. In the following section, we provide details on the spectrum sharing algorithm, including the alternating optimization of the above SDP problem.

V. Spectrum Sharing Algorithm

In this section, we summarize the roles played by the RS and CS for spectrum sharing in the considered two-tier model. Accordingly, we design a holistic algorithm as given in Algorithm 1 on top of next page, where Phase 2 of the algorithm is performed by the RS and Phase 3 takes place at the CS. Phase 1 of the algorithm, however, involves both CS and RS and is performed prior to Phase 2 and 3. Note that Phase 3 of the algorithm is iterative in nature and solves a SDP problem in each iteration, which makes it computationally intensive. Below we provide some qualitative analysis about Phase 3 of Algorithm 1.

1) Convergence of phase 3:

Proposition 2: The total MSE obtained after Sum-MSE minimization at CS monotonically decreases with respect to the iteration number n. Hence, Phase 3 of Algorithm 1 is convergent.

Proof: Let $\mathbf{MSE}^{UL} = \sum_{k=1}^{K} \mathbf{MSE}_k^{UL}$ and $\mathbf{MSE}^{DL} = \sum_{j=1}^{J} \mathbf{MSE}_j^{DL}$ denote the total MSE of the UL users and DL users, respectively. Thus, the total MSE of the CS can be defined as

$$\mathbf{MSE} = \sum\nolimits_{k=1}^{K} \mathbf{MSE}_k^{UL} + \sum\nolimits_{j=1}^{J} \mathbf{MSE}_j^{DL}. \tag{53}$$

For given $\mathbf{U}(n)$, $\mathbf{V}(n+1)$ can be computed at the $(n+1)^{th}$ iteration by solving the optimization problem **(P4)** and thus, we have following relation:

$$\mathbf{MSE}\left(\mathbf{V}(n+1), \mathbf{U}(n)\right) \leq \mathbf{MSE}\left(\mathbf{V}(n), \mathbf{U}(n)\right). \tag{54}$$

Similarly, for given $\mathbf{V}(n)$, we can update $\mathbf{U}(n+1)$ at the $(n+1)^{th}$ iteration by solving problem **(P4)**, yielding

$$\mathbf{MSE}\left(\mathbf{V}(n), \mathbf{U}(n+1)\right) \leq \mathbf{MSE}\left(\mathbf{V}(n), \mathbf{U}(n)\right). \tag{55}$$

From (54) and (55), we have

$$\mathbf{MSE}\left(\mathbf{V}(n+1), \mathbf{U}(n+1)\right) \leq \mathbf{MSE}\left(\mathbf{V}(n), \mathbf{U}(n)\right). \tag{56}$$

Now, from (54)-(56), we can observe that the total MSE of the CS decreases by updating the transmit precoding matrices (linear receiver matrices). Thus, the total MSE decreases monotonically and the Phase 3 of the algorithm is convergent, which concludes the proof. ∎

2) Computational complexity: The main complexity of the proposed spectrum sharing algorithm arises from Phase 3 (due to solving a SDP problem) at the CS, which depends on the number of arithmetic operations. In the following we evaluate its complexity.

Let $\mathbf{F}_i$ denotes a symmetric block-diagonal matrix, with D being the number of diagonal blocks of size $f_l \times f_l,\ l =$

Algorithm 1: Spectrum Sharing Algorithm for Coexistence between CS and RS

I. Phase 1 [Initial Phase]:
A: RS: Obtain CSI of $\{\mathbf{W}_i^{DL}, \forall i \in \mathcal{S}^{DL}, \mathbf{W}_{BR}^{DL}\}$.
B: RS: Set value for Γ.
C: CS: Obtain partial CSI of $\{\mathbf{G}_{RU_j}, \forall j \in \mathcal{S}^{UL}, \mathbf{G}_{RB}\}$.
D: CS: Set values for $P_0, P_i, \forall i \in \mathcal{S}^{UL}$.
E: If $(N_0(N_j) \neq R_r \,||\, \alpha_r \neq \alpha_c \,||\, \theta_t \neq \theta_c)\,\&\, R_T \gg (N_0 + JN_j)$, perform[8] Phase 2a.
F: Else if $(N_0(N_j) \neq R_r \,||\, \alpha_r \neq \alpha_c \,||\, \theta_t \neq \theta_c)\,\&\, R_T \ll (N_0 + JN_j)$, but $R_T > N_0$ and $R_T > N_j$, perform Phase 2b.
G: Else stop spectrum sharing until step E or F is satisfied.

II.1 Phase 2a [Precoder design at RS (Full mitigation)]:
A: Perform SVD of $\mathbf{W}$.
B: Construct $\bar{\mathbf{\Omega}}$ and $\tilde{\mathbf{\Omega}}$ and design the precoder matrix $\mathbf{P}$ based on (11).
C: Transmit $\mathbf{x}_R = \mathbf{P}\mathbf{s}_R$.

II.2 Phase 2b [Precoder design at RS (Partial mitigation)]:
A: Perform SVD of $\mathbf{W}_k,\ k \in \mathcal{I}$.
B: Calculate $k_{min} \triangleq \text{argmin}_{1 \leq k \leq \mathcal{I}} \parallel \mathbf{P}_k \mathbf{s}_R(l) - \mathbf{s}_R(l) \parallel_2$.
C: Define the precoder matrix as $\bar{\mathbf{P}} \triangleq \mathbf{P}_{k_{min}}$
D: Transmit $\mathbf{x}_R = \mathbf{P}\mathbf{s}_R$.

III. Phase 3 [Precoder design at CS]:
A: Set iteration number $n = 0$, maximum iteration number $= n_{max}$ and initialize $\mathbf{V}^{[n]}$ and $\mathbf{U}^{[n]}$.
B: $n \leftarrow n + 1$. For fixed $\mathbf{V}^{[n-1]}$, update $\mathbf{U}_i^{[n]},\ i \in \mathcal{S}$ by solving problem ($\mathbf{P4}$).
C: For fixed $\mathbf{U}^{[n]}$, update $\mathbf{V}_i^{[n]},\ i \in \mathcal{S}$ by solving problem (**P4**).
D: Repeat steps III.B and III.C until convergence or $n = n_{max}$.
E: Transmit $\mathbf{x}_i = \mathbf{V}_i \mathbf{s}_i\ i \in \mathcal{S}$.

$1, \ldots, D$. Then, the number of arithmetic operations required to solve a standard SDP problem of the form

$$\min_{\mathbf{t} \in \mathcal{R}^n} \quad \mathbf{c}^T \mathbf{t} \tag{57}$$

$$\text{subject to} \quad \mathbf{F}_0 + \sum\nolimits_{i=1}^{n} t_i \mathbf{F}_i \succeq \mathbf{0}, \text{ and } \quad \|\mathbf{t}\|_2 \leq T, \tag{58}$$

is upper-bounded by [32]

$$\mathcal{O}(1) \left(1 + \sum\nolimits_{l=1}^{D} f_l\right)^{1/2} n \left(n^2 + n \sum\nolimits_{l=1}^{D} f_l^2 + \sum\nolimits_{l=1}^{D} f_l^3\right). \tag{59}$$

Since an SDP problem is solved in Phase 3 of the proposed algorithm in two steps (Step III.B and Step III.C), the complexity for computing the optimal $\mathbf{V}_i$ and $\mathbf{U}_i$ can be found using (59) as follows. The number of diagonal blocks D in computing $\mathbf{V}_i$ is $|\mathcal{S}| + \left|\mathcal{S}^{UL}\right| + 2$, while the dimension of blocks is $f_i = A_i + \tilde{N}_i \tilde{M} + 1,\ i \in \mathcal{S}$ due to each user's MSE constraint. The UL user's and BS's power constraint make the blocks of size $f_i = \tilde{M} d_i^{UL} + 1,\ i \in \mathcal{S}^{UL}$ and $f_i = \tilde{M} \sum_{i \in \mathcal{S}^{DL}} d_i^{DL} + 1$, respectively. Additionally, $f = B + R\tilde{M} + 1$ owing to RS's interference constraint. The size of n is $\sum_{i \in \mathcal{S}} 2\tilde{M} d_i + 2|\mathcal{S}| + 1$ for computing all the unknown variables, wherein the term $\sum_{i \in \mathcal{S}} 2\tilde{M} d_i$ correlates with the real and image parts of $\mathbf{V}_i$ and the remaining terms are due to the additional slack variables. Similar to $\mathbf{V}_i$, we can also calculate the number of arithmetic operations required in finding the optimal $\mathbf{U}_i$, with $n = 2\tilde{N} d_i + 2,\ i \in \mathcal{S}$ and $f_i = A_i + \tilde{N}_i \tilde{M} + 1,\ i \in \mathcal{S}$.

3) Special case: One critical scenario for the concerned spectrum sharing framework is if $\mathbf{W} = \mathbf{Q}$, which arises when a BS (DL user) itself is a target for the radar and the following conditions are met.

$$N_0(N_j) = R_r \tag{60}$$

$$\alpha_r = \alpha_c \tag{61}$$

$$\theta_t = \theta_c. \tag{62}$$

Under such a scenario, since $\mathbf{W}\mathbf{x}_R(l) = \mathbf{0}$, therefore, $\mathbf{Q}\mathbf{x}_R(l) = \mathbf{0}$ and the radar will not be able to detect its target. However, this can be easily avoided by following any of the below mentioned guidelines.

- The RS has full CSI of the CS, i.e., the RS has full knowledge of $\mathbf{W}$. Hence, whenever $\mathbf{W} = \mathbf{Q}$, being the incumbent, the RS has the priority and can stop sharing its spectrum until $\mathbf{W} \neq \mathbf{Q}$, i.e., at least one of (60)–(62) is satisfied. This will guarantee the desired detection performance of the radar, but will push the violating cellular users that do not satisfy either of (60)–(62) into complete outage.
- The violating users can be served by moving them to non-radar frequency bands by using resource allocation and carrier aggregation techniques [35],
- Modify the MIMO RS's architecture as an overlapped-MIMO radar, where the transmit array of the colocated MIMO RS is partitioned into a number of subarrays that are allowed to overlap. The overlapped-MIMO RS architecture will then satisfy (60), thus increasing the DoF while mitigating interference to communication systems without sacrificing the main desirable characteristics for its own transmission [23].

Remark 5: Phase 1 of Algorithm 1 always checks if either of (60)–(62) is satisfied before Phase 2 and 3 are initiated, thus always ensuring that $\mathbf{W} \neq \mathbf{Q}$.

VI. Numerical Results

In this section, the performance of the proposed two-tier coexistence framework between a FD MU MIMO CS and a MIMO RS is evaluated through computer simulations[9] with respect to several elements, such as interference temperature towards RS from CS, transmitter/receiver distortion (measure of RSI) at CS, channel uncertainty size, CCI attenuation factor, number of antennas at the CS and RS, etc. The maximum number of iterations is set as 50 with tolerance value of 10^{-4}. The initialization points are selected using right singular matrices initialization [36] and the results are averaged over 100 independent channel realizations.

1) Simulation Setup: Motivated by FCC's proposal of using small cells in the 3.5 GHz band [37] we consider small cell

[9]For reference, the numerical results are obtained using MATLAB R2016b on a Linux server with Intel Xeon processor (16 cores, each clocked at 2 GHz) having 31.4 GiB of memory.

deployments under the 3GPP LTE specifications. Moreover, small cell, due to its low transmit power, short transmission distances and low mobility is considered suitable for FD technology [7]. Accordingly, a single hexagonal cell of radius $r = 40$ m is considered, where the FD BS[10] is located at the centre of the cell and the RS is located 400 m away from the circumference of the cell. The number of UL and DL users is set as $K = J = 2$ and each user, equipped equipped with N antennas is randomly located in the cell. For simplicity, we consider $M_0 = N_0 = N = \tilde{N}$. Next, to model the path loss in the CS, we consider the close-in (CI) free space reference distance path loss model as given in [38]. The CI model is a generic model that describes the large-scale propagation path loss at all relevant frequencies (> 2 GHz). This model can be easily implemented in existing 3GPP models by replacing a floating constant with a frequency-dependent constant that represents free space path loss in the first meter of propagation and is given as $PL(f,d) = PL_F(f,d_0) + 10\alpha_c \log_{10}(d/d_0) + \mathcal{X}_\sigma$, $d > d_0$. Here, d_0 is a reference distance at which or closer to, the path loss inherits the characteristics of free-space path loss PL_F. Further, f is the carrier frequency, α_c is the path loss exponent, d is the distance between the transmitter and receiver and $\mathcal{X}_\sigma$ is the shadow fading standard deviation. We consider $d_0 = 1$ m, $B = 100$ MHz, and carrier frequency $= 3.6$ GHz[11].

The estimated channel gain between the BS and kth UL user can be described as $\tilde{\mathbf{H}}_k^{UL} = \sqrt{\wp_k^{UL}}\hat{\mathbf{H}}_k^{UL}$, where $\hat{\mathbf{H}}_k^{UL}$ denotes small scale fading following a complex Gaussian distribution with zero mean and unit variance, and $\wp_k^{UL} = 10^{(-\mathrm{A}/10)}$, $A \in \{\mathrm{LOS}, \mathrm{NLOS}\}$[12] denotes the large scale fading consisting of path loss and shadowing. LOS and NLOS are computed based on a street canyon scenario [39]. The parameter α_c for LOS and NLOS are set as 2.0 and 3.1, respectively, while the value of shadow fading standard deviation σ for LOS and NLOS are 2.9 dB and 8.1 dB, respectively. Similarly, we define the channels between UL users and DL users, between BS and DL users, between BS and radar, and between UL users and radar. To model the SI channel, the Rician model in [8] is adopted, wherein the SI channel is distributed as $\tilde{\mathbf{H}}_0 \sim \mathcal{CN}\left(\sqrt{\frac{K_R}{1+K_R}}\hat{\mathbf{H}}_0, \frac{1}{1+K_R}\mathbf{I}_{N_0} \otimes \mathbf{I}_{M_0}\right)$, where K_R is the Rician factor and $\hat{\mathbf{H}}_0$ is a deterministic matrix[13]. Unless otherwise stated, we take into account the full mitigation scenario as described in section III.A.1 and consider the following parameters for the CS and RS. For CS: thermal noise density $= -174$ dBm/Hz, noise figure at BS (users) 13(9) dB, $\tilde{N} = 2$, $\psi = \upsilon = -70$ dB, $\delta = \hat{\varrho} = 0.1$, $P_i = 5$ dB, $P_0 = 10$ dB, and CCI cancellation factor[14]$= 0.3$. For RS:

[10]The BS has total $N_0 + M_0$ antennas. However, when BS operates in HD mode, it uses only M_0 (N_0) antennas for transmission (reception) [29].

[11]The framework presented in this paper is not limited to any particular frequency band and can also be utilized in other spectrums proposed for sharing around the world, such as 2-4 GHz in the UK, 2.3-2.4 GHz in Europe, etc., albeit with certain changes in frequency dependent path loss, line of sight propagation parameters, etc.

[12]LOS=Line-of-sight and NLOS=Non-line-of-sight.

[13]For simplicity, we consider $K_R = 1$ and the matrix $\tilde{\mathbf{H}}_0$ of all ones for all simulations [40].

[14]Details on CCI cancellation is provided in the explanation of Fig. 7.

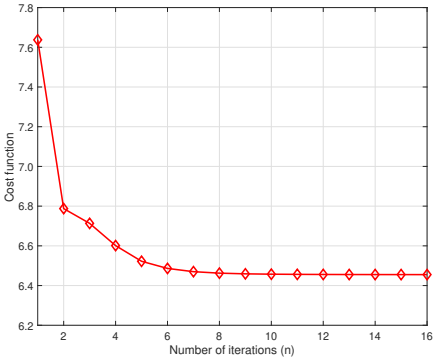

Fig. 3: Convergence of the proposed algorithm.

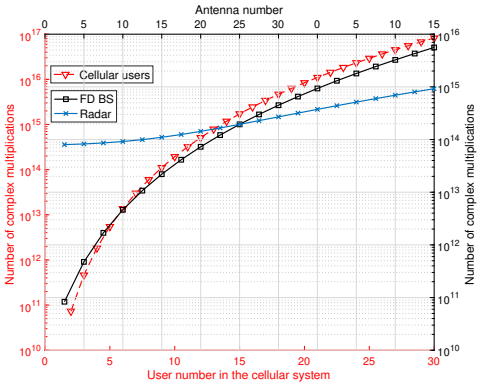

Fig. 4: Complexity of the proposed algorithm for $n = 1$.

$R = 8$, $P_{FA} = 10^{-5}$, $\Gamma = 0$ dB, velocity of target $= 782$ knots, and distance of target from RS $= 300$ m.

2) Simulation Results: After the completion of Phase 1 of Algorithm 1, RS deploys Phase 2 to null the interference from RS $\rightarrow$ CS, i.e., $\mathbf{W}_i\mathbf{x}_R = \mathbf{0}, i \in \mathcal{I}$, which is then followed by the deployment of Phase 3 at CS to suppress the interference from CS $\rightarrow$ RS and also provide data throughput to its users[15]. In the following examples, we illustrate the performance of both RS and CS utilizing Phase 2 and 3 of the proposed algorithm. Due to the iterative nature of Phase 3 of the algorithm, we begin by showing 1) its evolution in Fig. 3, i.e., its convergence in terms of the number of iterations required (n) and 2) its complexity analysis in Fig. 4 in terms of complex multiplications required with respect to (w.r.t) increasing number of antennas at CS and RS and users in the CS. Accordingly, it can be seen from Fig. 3 that the cost function (sum-MSE) monotonically decreases and converges between $n = 10$ and $n = 14$, which verifies the proof of Theorem 2. Similar to other iteration algorithms' performance, the value of n depends on the intitalization states of the channels in consideration. Further, in Fig. 4, it can be seen that the computational complexity of Phase 3 of the algorithm increases as the number of users or antennas are increased. The axes in red (left and bottom) represent the complexity w.r.t number of users while the axes in black (right and top) represent the complexity w.r.t number of antennas at radar and BS. Hence, the processing of Phase 3 of the algorithm

[15]Note that the three phases of Algorithm 1 must be processed within the same coherence time interval.

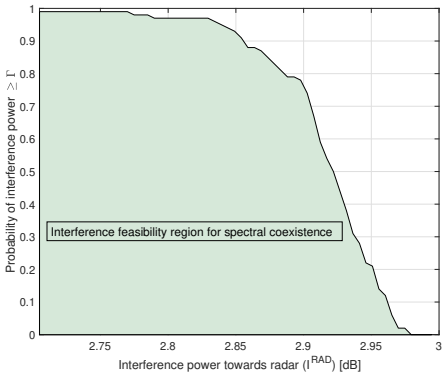

Fig. 5: Probability of interference power from CS to RS w.r.t maximum allowed interference temperature, Γ.

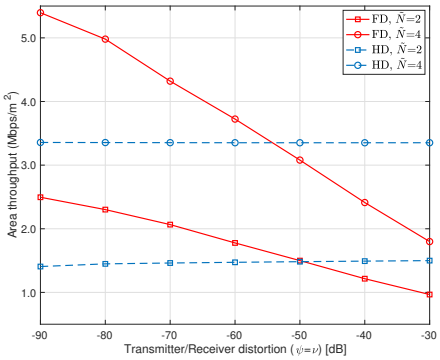

Fig. 6: Sum rate of FD CS vs. hardware impairment at FD BS.

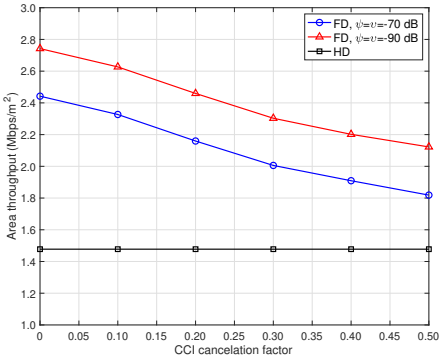

Fig. 7: Sum rate of FD CS vs. various CCI cancellation factors.

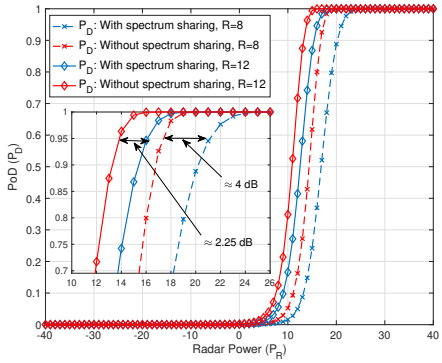

Fig. 8: Detection probability (P_D) vs. radar transmit power (P_R).

should be handled centrally at the FD BS, which inadvertently has high end computing capabilities. Note that Fig. 4 is generated for $n = 1$. To incorporate the effect of the alternating optimization, the computational complexity calculated for one iteration can be multiplied with the exact value of n, which is obtained in Fig. 3.

Next, we quantify the performance of the CS (operating in the spectrum shared by the RS) in terms of area throughput[16] (Mbps/m^2). However, prior to that, in order to verify that Phase 3 of Algorithm 1 does not violate the interference temperature set by the RS in Phase 1, we show the complementary cumulative distribution (CCD) of the total interference power from the CS to RS, i.e., $\mathbb{P}[I^{RAD} \leq \Gamma]$. For this example, we set the maximum allowed total interfering power at 3 dB. It can be seen from Fig. 5 that the probability of total interference power from the CS to the RS is zero when it is close to or higher than $\Gamma = 3$ dB. This verifies the operation of Phase 3 of the algorithm, which ensures that the interference to the radar is always kept below or equal to the interference temperature preset by the RS during Phase 1. While achieving equality will ensure maximum throughput for the CS, the proposed Phase 3 mainly operates below the interference temperature to protect the RS, but still providing the users of the CS with specific QoS, which we quantify in the next example. Further, the area under the CCD curve can be contemplated as the region, under which Phase 3 of the algorithm is always feasible to enable the coexistence between RS and CS.

In Fig. 6, we show the area throughput of the CS as a function of transmitter/receiver (ψ/υ) distortion values for different number of antennas, which is obtained by minimizing the sum-MSE of the CS in Phase 3 of the algorithm. The transmitter/receiver distortion reflects the amount of RSI in the FD system. It can be seen from the figure that as the RSI cancellation capability of the system increases, the throughput achieved by the FD system also increases. However, the performance of the HD system is invariant to ψ and υ values. In particular FD achieves around $40 - 50\%$ improvement in throughput over HD at a reasonable RSI of -70 dB. However, at low RSI cancellation levels (i.e., ≤ -50 dB), the distortion is magnified with the increasing number of antennas and the HD system starts outperforming the FD system. Similarly, in Fig. 7, we show the effect of isolation (CCI attenuation) among the UL and DL users on the performance of the FD system. It can be seen that as the level of CCI cancellation increases (0 representing 100% cancellation and 1 representing no cancellation), the FD system starts outperforming the HD system considerably. Hence, smart channel assignment, at a stage prior to the precoder/decoder design is essential to create isolation among the UL and DL users for a successful coexistence of UL and DL users in the FD system. This can be done by clustering the users into different groups through techniques, such as game theory, where the users with very strong CCI are not placed in the same group.

To detect a target in the far-field, the RS transmits precoded

[16]The area throughput of the FD MU MIMO CS can be calculated as $\frac{B}{\tau^2}\sum_{i\in\mathcal{S}}\sum_{k=1}^{d_i}\log_2\left(1+\mathrm{SINR}_{i_k}\right)$, where $\mathrm{SINR}_{i_k} = \frac{\mathbf{u}_{i_k}^H\mathbf{H}_{ii}\mathbf{v}_{i_k}\mathbf{v}_{i_k}^H\mathbf{H}_{ii}^H\mathbf{u}_{i_k}}{\mathbf{u}_{i_k}^H\left(\mathbf{\Sigma}_i+\sum_{j\neq k}\mathbf{H}_{ii}\mathbf{v}_{i_j}\mathbf{v}_{i_j}^H\mathbf{H}_{ii}^H\right)\mathbf{u}_{i_k}}$. Here, $\mathbf{u}_{i_k}$ and $\mathbf{v}_{i_k}$ are the k-th column of $\mathbf{U}_i$, and $\mathbf{V}_i$, respectively.

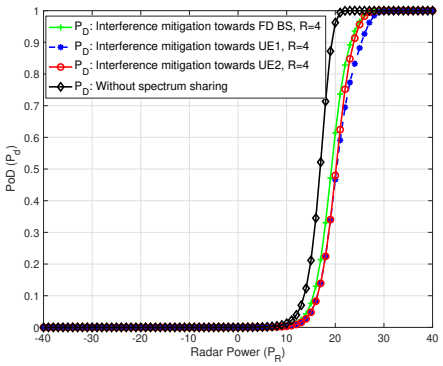

Fig. 9: Detection probability (P_D) vs. radar transmit power (P_R) for partial mitigation.

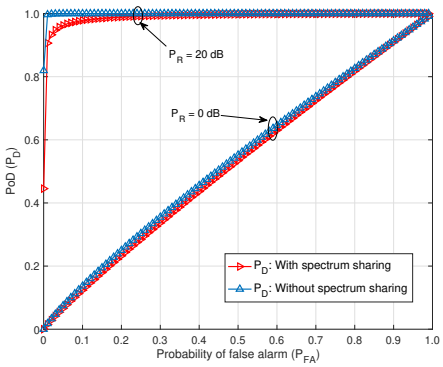

Fig. 10: Detection probability (P_D) vs. probability of false alarm (P_{FA}).

waveforms generated in Phase 2 of the algorithm and estimates parameters θ and α_r from the received signal (also involving I^{RAD}, which is obtained from Phase 3 of the algorithm). As a benchmark, we also simulate the scenario without spectrum sharing by generating orthogonal waveforms at the RS and setting $I^{RAD} = 0$, which signifies that the throughput of CS is zero with no coverage.

We begin by showing the detection probability of the MIMO RS w.r.t. RS's transmit power in Fig. 8. We consider two cases here: 1) $R = 12$ (straight lines) and $R = 8$ (dashed lines). It can be seen that for fixed P_{FA}, in order to achieve a particular P_D the radar needs more power (to mitigate interference towards CS and withstand interference from CS to enable spectrum coexistence) than the case without spectrum sharing scenario. However, it can be seen that the RS needs more power when $R = 8$ than $R = 12$ to achieve similar performance. This is because, while the number of antennas at the CS (BS and users) are fixed, increasing the radar antennas means that it has more degrees of freedom for reliable target detection and simultaneously nulling out interference towards the CS. This proves that large antenna arrays at the RS can be used to facilitate spectrum sharing without any degradation in radar's performance. Furthermore, for the case of partial interference mitigation as was described in section III.A.2, we show the detection probability performance of the RS in Fig. 9, when $R_T << (N_0 + JN_j)$, but $R_T > N_0$ and $R_T > N_j$. Here, we consider $R_T = 4$, which is less than $N_0 + JN_j = 6$, but greater than $\tilde{N} = 2$.

Next, in Fig. 10, we plot PoD for various P_{FA} and P_R. This figure shows the gap in performance with and without spectrum sharing for two different transmit powers of RS. The area of interest here is the region below $P_{FA} = 10^{-3}$. Similar to the previous figure, it can be seen that at $P_R = 20$dB, spectrum sharing does not affect the performance of the MIMO RS too much, as it is quite comparable to the case without sharing.

Finally, to summarize, we show the explicit tradeoff between the performance of RS and CS in Fig. 11. Accordingly, it can be seen from Fig. 11.a, that as the interference threshold increases the area throughput of the cellular system also increases. This is due to the fact increasing the interference threshold allows the UL users and the BS to operate at higher transmit power regime to obtain higher area throughput. However, as a consequence, the PoD of the radar decreases, which is seen from Fig. 11.b. Nevertheless, for the case of $\Gamma = 0$ dB and $P_{FA} = 10^{-5}$, as has been considered in Fig. 6 and Fig. 7 in the manuscript, it can be seen that PoD is equal to 0.978. This performance is quite reasonable considering the fact that spectrum sharing is usually associated with assorted benefits, that can be mutually agreed upon between federal authorities and cellular operators in prior.

VII. Conclusions

Precoders were designed at MIMO RS and FD MU MIMO CS to facilitate a QoS incentivized two-tier spectrum sharing framework. Numerical results demonstrated the effectiveness of the proposed spectrum sharing algorithm to tackle the imperfect nature of wireless channels and hardwares at the CS, albeit with certain tradeoffs in radar transmit power, PoD and QoS of the cellular users. In particular, using the spectrum shared by the RS, the FD CS was able to achieve an area throughput of around $4 - 5$ Mbps/m^2 for a reasonable SI cancellation of around -70 dB. However, to facilitate this, while also maintaining a detection probability of around 0.9, the radar was required to spend an extra power of around $2-4$ dB, depending on the number of antennas at the RS.

Appendix A: Useful Lemmas

Lemma 5: (Sign-definiteness Lemma [34]) For matrices $\mathbf{P}$, $\mathbf{Q}$, and $\mathbf{A}$, with $\mathbf{A} = \mathbf{A}^H$, the semi-infinite LMI of the form $\mathbf{A} \succeq \mathbf{P}^H\mathbf{X}\mathbf{Q} + \mathbf{Q}^H\mathbf{X}^H\mathbf{P}, \forall \mathbf{X} : \|\mathbf{X}\|_F \leq \rho$, holds *iff* $\exists \epsilon \geq 0$ such that

$$\begin{bmatrix} \mathbf{A} - \epsilon\mathbf{Q}^H\mathbf{Q} & -\rho\mathbf{P}^H \\ -\rho\mathbf{P} & \epsilon\mathbf{I} \end{bmatrix} \succeq 0. \tag{63}$$

The proof is obtained by emplying the combination of the Cauchy-Schwarz inequality, together with the well-known S-procedure on the semi-infinite LMI, please see [34, Lemma 1] for the details.

Appendix B: Proof of Lemma 3

Since $\mathbf{A}(\theta)\bar{\mathbf{P}}\bar{\mathbf{P}}^H\mathbf{A}^H(\theta)$ and $\hat{\boldsymbol{\chi}}$ are positive-definite, we have

$$\text{tr}\left(\mathbf{A}(\theta)\bar{\mathbf{P}}\bar{\mathbf{P}}^H\mathbf{A}^H(\theta)\hat{\boldsymbol{\chi}}^{-1}\hat{\boldsymbol{\chi}}\right) \leq \text{tr}\left(\mathbf{A}(\theta)\bar{\mathbf{P}}\bar{\mathbf{P}}^H\mathbf{A}^H(\theta)\hat{\boldsymbol{\chi}}^{-1}\right)\text{tr}(\hat{\boldsymbol{\chi}}), \tag{64}$$

$$\implies \text{tr}\left(\mathbf{A}(\theta)\bar{\mathbf{P}}\bar{\mathbf{P}}^H\mathbf{A}^H(\theta)\hat{\boldsymbol{\chi}}^{-1}\right) \geq \frac{\text{tr}\left(\mathbf{A}(\theta)\mathbf{A}^H(\theta)\right)\text{tr}\left(\bar{\mathbf{P}}\bar{\mathbf{P}}^H\right)}{\text{tr}(\hat{\boldsymbol{\chi}})}. \tag{65}$$

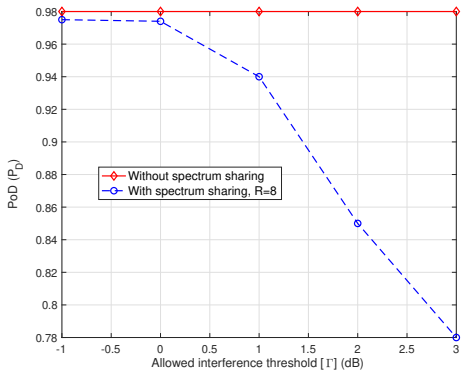

(a) RS: Allowed interference temperature (Γ) vs PoD (P_D) of radar.

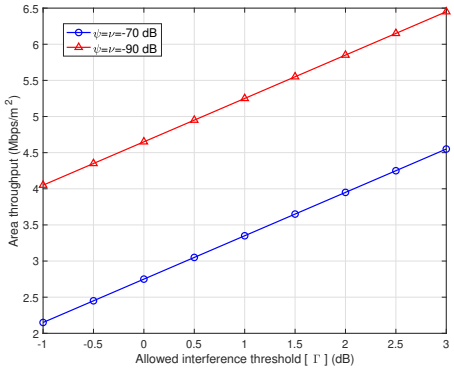

(b) CS: Allowed interference temperature (Γ) vs. area throughput of CS.

Fig. 11: Performance tradeoff between RS and CS.

Now, since $\hat{\boldsymbol{\chi}} = \tilde{\boldsymbol{\chi}} + \sigma_R^2 \mathbf{I}_R$ and for $R_T = R_R = R$, we have $\text{tr}\left(\mathbf{A}(\theta)\mathbf{A}(\theta)^H\right) = R^2$, (65) can be rewritten as

$$\text{tr}\left(\mathbf{A}(\theta)\bar{\mathbf{P}}\bar{\mathbf{P}}^H\mathbf{A}^H(\theta)\hat{\boldsymbol{\chi}}^{-1}\right) \geq \frac{R^2\varphi}{\text{tr}(\tilde{\boldsymbol{\chi}}) + \text{tr}(\sigma_R^2\mathbf{I}_R)} = \frac{\varphi R^2}{I^{RAD} + R\sigma_R^2}, \tag{66}$$

where $\varphi = \text{tr}(\bar{\mathbf{P}}\bar{\mathbf{P}}^H)$.

Appendix C: Proof of Lemma 4

From (37), $\text{tr}\{\mathbf{MSE}_i\}$ is given by

$$\begin{aligned}
\text{tr}\{\mathbf{MSE}_i\} &= \text{tr}\left\{\left(\mathbf{U}_i^H\mathbf{H}_{ii}\mathbf{V}_i - \mathbf{I}_{d_i}\right)\left(\mathbf{U}_i^H\mathbf{H}_{ii}\mathbf{V}_i - \mathbf{I}_{d_i}\right)^H\right\} \\
&+ \sum\nolimits_{j\in\mathcal{S}, j\neq i} \text{tr}\left\{\mathbf{U}_i^H\mathbf{H}_{ij}\mathbf{V}_j\mathbf{V}_j^H\mathbf{H}_{ij}^H\mathbf{U}_i\right\} \\
&+ \sum\nolimits_{j\in\mathcal{S}}\sum\nolimits_{\ell\in\mathcal{D}_j^{(\tilde{M})}} \psi\,\text{tr}\left\{\mathbf{U}_i^H\mathbf{H}_{ij}\boldsymbol{\Xi}_\ell\mathbf{V}_j\mathbf{V}_j^H\boldsymbol{\Xi}_\ell^H\mathbf{H}_{ij}^H\mathbf{U}_i\right\} \\
&+ \sum\nolimits_{j\in\mathcal{S}}\sum\nolimits_{\ell\in\mathcal{D}_i^{(\tilde{N})}} \upsilon\,\text{tr}\left\{\mathbf{U}_i^H\boldsymbol{\Xi}_\ell\mathbf{H}_{ij}\mathbf{V}_j\mathbf{V}_j^H\mathbf{H}_{ij}^H\boldsymbol{\Xi}_\ell^H\mathbf{U}_i\right\}, \\
&+ P_R\text{tr}\left\{\mathbf{U}_i^H\mathbf{W}_i(\mathbf{W}_i)^H\mathbf{U}_i\right\} + \sigma_i^2\text{tr}\left\{\mathbf{U}_i^H\mathbf{U}_i\right\}
\end{aligned} \tag{67}$$

where $\boldsymbol{\Xi}_\ell$ is a square matrix with zero elements, except for the ℓ-th diagonal element, which is equal to 1. The symbols $\mathcal{D}_j^{(\tilde{N})}$ and $\mathcal{D}_j^{(\tilde{M})}$ indicate the set $\{1\cdots\tilde{N}_j\}$ and $\{1\cdots\tilde{M}_j\}$, respectively. Using $\|\text{vec}(\mathbf{A})\|_2^2 = \text{tr}\{\mathbf{A}\mathbf{A}^H\}$ and the vec$(\cdot)$ operation, (67) is re-expressed as

$$\begin{aligned}
\text{tr}\{\mathbf{MSE}_i\} &= \left\|\text{vec}\left(\mathbf{U}_i^H\mathbf{H}_{ii}\mathbf{V}_i\right) - \text{vec}(\mathbf{I}_{d_i})\right\|_2^2 \\
&+ \sum_{j\in\mathcal{S}, j\neq i}\left\|\text{vec}\left(\mathbf{U}_i^H\mathbf{H}_{ij}\mathbf{V}_j\right)\right\|_2^2 + P_R\left\|\text{vec}\left(\mathbf{U}_i^H\mathbf{W}_i\right)\right\|_2^2 \\
&+ \sum_{j\in\mathcal{S}}\sum_{\ell\in\mathcal{D}_j^{(\tilde{M})}} \psi\left\|\text{vec}\left(\mathbf{U}_i^H\mathbf{H}_{ij}\boldsymbol{\Xi}_\ell\mathbf{V}_j\right)\right\|_2^2
\end{aligned} \tag{68}$$

$$+ \sum_{j\in\mathcal{S}}\sum_{\ell\in\mathcal{D}_i^{(\tilde{N})}} \upsilon\left\|\text{vec}\left(\mathbf{U}_i^H\boldsymbol{\Xi}_\ell\mathbf{H}_{ij}\mathbf{V}_j\right)\right\|_2^2 + \sigma_i^2\left\|\text{vec}\left(\mathbf{U}_i^H\right)\right\|_2^2$$

Now, using $\text{vec}(\mathbf{ABC}) = \left(\mathbf{C}^T\otimes\mathbf{A}\right)\text{vec}(\mathbf{B})$, (68) can be rewritten as $\|\boldsymbol{\mu}_i\|_2^2$, where $\boldsymbol{\mu}_i$ is defined in (44). In a similar manner, I^{RAD} can also be rewritten as

$$I^{RAD} = \sum\nolimits_{j\in\mathcal{S}}\left(\|\text{vec}(\mathbf{G}_{lj}\mathbf{V}_j)\|_2^2 + \sum\nolimits_{\ell\in\mathcal{D}_j^{(\tilde{M})}}\psi\|\text{vec}(\mathbf{G}_{lj}\boldsymbol{\Xi}_\ell\mathbf{V}_j)\|_2^2\right), \tag{69}$$

and can be expressed as $\|\boldsymbol{\iota}\|_2^2$, wherein $\boldsymbol{\iota}$ is given in (45).

Appendix D: Proof of Proposition 1

Using the vector forms from (44) and (45), the optimization problem **(P3)** is reformulated as

$$\begin{aligned}
\textbf{(P3.A)} \quad & \min_{\mathbf{V},\mathbf{U},\boldsymbol{\tau}} \sum\nolimits_{i\in\mathcal{S}}\tau_i \\
\text{s.t } (C.1) \quad & \|\boldsymbol{\mu}_i\|_2^2 \leq \tau_i,\ \|\boldsymbol{\Delta}_i\|_F \leq \delta_i,\ i\in\mathcal{S}, \\
(C.2) \quad & \|\text{vec}(\mathbf{V}_i)\|_2^2 \leq P_i,\ i\in\mathcal{S}^{UL}, \\
(C.3) \quad & \|\lfloor\text{vec}(\mathbf{V}_i)\rfloor_{i\in\mathcal{S}^{DL}}\|_2^2 \leq P_0, \\
(C.4) \quad & \|\boldsymbol{\iota}\|_2^2 \leq \Gamma,\ \|\boldsymbol{\Lambda}\|_F \leq \hat{\varrho}.
\end{aligned} \tag{70}$$

The constraints $(C.1)$ and $(C.4)$ above are not in LMI form. Therefore, to transform the semi-infinite problem **(P3.A)** into a SDP problem, we use the Schur complement lemma to rewrite the constraints $(C.1)$ and $(C.4)$ into LMI forms. Thus, the new optimization problem can be given as

$$\begin{aligned}
\textbf{(P3.B)} \quad & \min_{\mathbf{V},\mathbf{U},\boldsymbol{\tau}} \sum\nolimits_{i\in\mathcal{S}}\tau_i \\
\text{s.t } (C.1) \quad & \begin{bmatrix}\tau_i & \boldsymbol{\mu}_i^H \\ \boldsymbol{\mu}_i & \mathbf{I}_{A_i}\end{bmatrix} \succeq 0,\ \|\boldsymbol{\Delta}_i\|_F \leq \delta_i,\ i\in\mathcal{S}, \\
(C.2) \quad & \|\text{vec}(\mathbf{V}_i)\|_2^2 \leq P_i,\ i\in\mathcal{S}^{UL} \\
(C.3) \quad & \|\lfloor\text{vec}(\mathbf{V}_i)\rfloor_{i\in\mathcal{S}^{DL}}\|_2^2 \leq P_0\,, \\
(C.4) \quad & \begin{bmatrix}\Gamma & \boldsymbol{\iota}^H \\ \boldsymbol{\iota} & \mathbf{I}_B\end{bmatrix} \succeq 0,\ \|\boldsymbol{\Lambda}\|_F \leq \hat{\varrho},
\end{aligned} \tag{71}$$

where the identity matrices in $(C.1)$ and $(C.3)$ have the following dimensions

$$\begin{aligned}
A_i &= d_i\left(\sum\nolimits_{j\in\mathcal{S}}\left(d_j + \tilde{M}_j\right) + \tilde{N}_i\right) + \tilde{N}_i\sum\nolimits_{j\in\mathcal{S}} d_j, \\
\text{and } \ B &= R\sum\nolimits_{j\in\mathcal{S}}\left(d_j + \tilde{M}_j\right).
\end{aligned} \tag{72}$$

Using Lemma 5, we can further simplify the problem **(P3.B)** by relaxing the semi-infiniteness of the constraints $(C.1)$ and $(C.3)$. The estimated channel and the channel estimation error are required to be separated before applying Lemma 5. Thus, we first express the LMI in $(C.1)$ as

$$\begin{bmatrix}\tau_i & \tilde{\boldsymbol{\mu}}_i^H \\ \tilde{\boldsymbol{\mu}}_i & \mathbf{I}_{A_i}\end{bmatrix} + \begin{bmatrix}0 & \boldsymbol{\mu}_{\Delta_i}^H \\ \boldsymbol{\mu}_{\Delta_i} & \mathbf{0}_{A_i\times A_i}\end{bmatrix} \succeq 0, \tag{73}$$

where

$$\tilde{\boldsymbol{\mu}}_i = \begin{bmatrix} \left(\mathbf{V}_i^T \otimes \mathbf{U}_i^H\right) \mathrm{vec}\left(\tilde{\mathbf{H}}_{ii}\right) - \mathrm{vec}\left(\mathbf{I}_{d_i}\right) \\ \left\lfloor \left(\mathbf{V}_j^T \otimes \mathbf{U}_i^H\right) \mathrm{vec}\left(\tilde{\mathbf{H}}_{ij}\right) \right\rfloor_{j\in\mathcal{S}, j\neq i} \\ \left\lfloor \left\lfloor \sqrt{\psi} \left((\boldsymbol{\Xi}_\ell \mathbf{V}_j)^T \otimes \mathbf{U}_i^H\right) \mathrm{vec}\left(\tilde{\mathbf{H}}_{ij}\right) \right\rfloor_{\ell\in\mathcal{D}_j^{(\tilde{M})}} \right\rfloor_{j\in\mathcal{S}} \\ \left\lfloor \left\lfloor \sqrt{\upsilon} \left(\mathbf{V}_j^T \otimes (\mathbf{U}_i^H \boldsymbol{\Xi}_\ell)\right) \mathrm{vec}\left(\tilde{\mathbf{H}}_{ij}\right) \right\rfloor_{\ell\in\mathcal{D}_i^{(\tilde{N})}} \right\rfloor_{j\in\mathcal{S}} \\ P_R \left(\mathbf{I}_R^T \otimes \mathbf{U}_i^H\right) \mathrm{vec}\left(\mathbf{W}_i\right) \\ \sigma_i \mathrm{vec}\left(\mathbf{U}_i\right) \end{bmatrix},$$

$$\boldsymbol{\mu}_{\Delta_i} = \underbrace{\begin{bmatrix} \left(\mathbf{V}_i^T \otimes \mathbf{U}_i^H\right) \\ \left\lfloor \left(\mathbf{V}_j^T \otimes \mathbf{U}_i^H\right) \right\rfloor_{j\in\mathcal{S}, j\neq i} \\ \left\lfloor \left\lfloor \sqrt{\psi} \left((\boldsymbol{\Xi}_\ell \mathbf{V}_j)^T \otimes \mathbf{U}_i^H\right) \right\rfloor_{\ell\in\mathcal{D}_j^{(\tilde{M})}} \right\rfloor_{j\in\mathcal{S}} \\ \left\lfloor \left\lfloor \sqrt{\upsilon} \left(\mathbf{V}_j^T \otimes (\mathbf{U}_i^H \boldsymbol{\Xi}_\ell)\right) \right\rfloor_{\ell\in\mathcal{D}_i^{(\tilde{N})}} \right\rfloor_{j\in\mathcal{S}} \\ \mathbf{0}_{d_i \tilde{N}_i \times \tilde{N}_i \tilde{M}} \\ \mathbf{0}_{d_i \tilde{N}_i \times \tilde{N}_i \tilde{M}} \end{bmatrix}}_{\mathbf{D}_{\Delta_i}} \mathrm{vec}\left(\boldsymbol{\Delta_i}\right).$$

By selecting

$$\mathbf{A} = \begin{bmatrix} \tau_i & \tilde{\boldsymbol{\mu}}_i^H \\ \tilde{\boldsymbol{\mu}}_i & \mathbf{I}_{A_i} \end{bmatrix}, \ \mathbf{P} = \left[\mathbf{0}_{\tilde{N}_i \tilde{M} \times 1}, \ \mathbf{D}_{\Delta_i}^H\right], \\ \mathbf{X} = \mathrm{vec}\left(\boldsymbol{\Delta_i}\right), \ \mathbf{Q} = \left[-1, \mathbf{0}_{1\times A_i}\right], \tag{74}$$

and using Lemma 5, we relax the LMI in $(C.1)$ as

$$\begin{bmatrix} \tau_i - \epsilon_i & \tilde{\boldsymbol{\mu}}_i^H & \mathbf{0}_{1\times \tilde{N}_i \tilde{M}} \\ \tilde{\boldsymbol{\mu}}_i & \mathbf{I}_{A_i} & -\delta_i \mathbf{D}_{\Delta_i} \\ \mathbf{0}_{\tilde{N}_i \tilde{M}\times 1} & -\delta_i \mathbf{D}_{\Delta_i}^H & \epsilon_i \mathbf{I}_{\tilde{N}_i \tilde{M}} \end{bmatrix} \succeq 0, \epsilon_i \geq 0, i \in \mathcal{S}. \tag{75}$$

Similarly, we can also express the LMI in $(C.3)$ as

$$\begin{bmatrix} \Gamma & \tilde{\boldsymbol{\iota}}^H \\ \tilde{\boldsymbol{\iota}} & \mathbf{I}_B \end{bmatrix} + \begin{bmatrix} 0 & \boldsymbol{\iota}_\Lambda^H \\ \boldsymbol{\iota}_\Lambda & \mathbf{0}_{B\times B} \end{bmatrix} \succeq 0, \tag{76}$$

where

$$\tilde{\boldsymbol{\iota}} = \begin{bmatrix} \left\lfloor \left(\mathbf{V}_j^T \otimes \mathbf{I}_T\right) \mathrm{vec}\left(\tilde{\mathbf{G}}_{lj}\right) \right\rfloor_{j\in\mathcal{S}} \\ \sqrt{\psi} \left\lfloor \left\lfloor \left((\boldsymbol{\Xi}_\ell \mathbf{V}_j)^T \otimes \mathbf{I}_T\right) \mathrm{vec}\left(\tilde{\mathbf{G}}_{lj}\right) \right\rfloor_{\ell\in\mathcal{D}_j^{(\tilde{M})}} \right\rfloor_{j\in\mathcal{S}} \end{bmatrix}, \tag{77}$$

$$\boldsymbol{\iota}_\Lambda = \underbrace{\begin{bmatrix} \left\lfloor \left(\mathbf{V}_j^T \otimes \mathbf{I}_R\right) \right\rfloor_{j\in\mathcal{S}} \\ \sqrt{\psi} \left\lfloor \left\lfloor \left((\boldsymbol{\Xi}_\ell \mathbf{V}_j)^T \otimes \mathbf{I}_R\right) \right\rfloor_{\ell\in\mathcal{D}_j^{(\tilde{M})}} \right\rfloor_{j\in\mathcal{S}} \end{bmatrix}}_{\mathbf{E}_\Lambda} \mathrm{vec}\left(\boldsymbol{\Lambda}\right), \tag{78}$$

and the relaxed form of the LMI in $(C.3)$ is written as

$$\begin{bmatrix} \Gamma - \eta & \tilde{\boldsymbol{\iota}}^H & \mathbf{0}_{1\times R\tilde{M}} \\ \tilde{\boldsymbol{\iota}} & \mathbf{I}_B & -\hat{\varrho}\mathbf{E}_\Lambda \\ \mathbf{0}_{R\tilde{M}\times 1} & -\hat{\varrho}\mathbf{E}_\Lambda^H & \eta \mathbf{I}_{R\tilde{M}} \end{bmatrix} \succeq 0, \ \eta \geq 0. \tag{79}$$

From (75) and (79), we can rewrite **(P3)** as an equivalent SDP problem as given in **(P4)**.

REFERENCES

[1] Federal Communications Commission (FCC), Spectrum policy task force, [Online] Available: https://transition.fcc.gov/sptf/files/IPWGFinalReport.pdf, Nov. 2002.

[2] National Telecommunications and Information Administration (NTIA), An assessment of the near-term viability of accommodating wireless broadband systems in the 1675-1710 MHz, 1755-1780 MHz, 3500-3650 MHz, 4200-4220 MHz, and 4380-4400 MHz bands (Fast track report), [Online] Available: https://www.ntia.doc.gov/files/ntia/publications/fasttrackevaluation_11152010.pdf, Nov. 2010.

[3] S. Haykin, "Cognitive radio: Brain-empowered wireless communications," *IEEE J. Sel. Areas Commun.*, vol. 23, no. 2, pp. 201-220, Feb. 2005.

[4] B. P. Day, A. R. Margetts, D. W. Bliss, and P. Schniter, "Full-duplex bidirectional MIMO: Achievable rates under limited dynamic range," *IEEE Trans. Signal Process.*, vol. 60, no. 7, pp. 3702-3713, Jul. 2012.

[5] A. C. Cirik, S. Biswas, S. Vuppala, and T. Ratnarajah, "Robust transceiver design for full duplex multiuser MIMO systems," *IEEE Wireless Commun. Lett.*, vol. 5, no. 3, pp. 260-263, Jun. 2016.

[6] A. C. Cirik, S. Biswas, S. Vuppala, and T. Ratnarajah, "Beamforming Design for full-duplex MIMO interference channels-QoS and energy-efficiency considerations," *IEEE Trans. Commun.*, vol. 64, no. 11, pp. 4635-4651, Nov. 2016.

[7] A. C. Cirik, S. Biswas, S. O. Taghizadeh, and T. Ratnarajah, "Robust transceiver design in full-duplex MIMO cognitive radios," *IEEE Trans. Veh. Technol.*, vol. PP, no. 99, pp. 1-1, 2017.

[8] M. Duarte, C. Dick, and A. Sabharwal, "Experiment-driven characterization of full-duplex wireless systems," *IEEE Trans. Wireless Commun.*, vol. 11, no. 12, pp. 4296-4307, Dec. 2012.

[9] M. J. Marcus, "New approaches to private sector sharing of federal government spectrum," *New Amer. Found.*, no. 26, pp. 1-8, Jun. 2009.

[10] S.-S. Raymond, A. Abubakari, and H.-S. Jo, "Coexistence of power-controlled cellular networks with rotating radar," *IEEE J. Sel. Areas Commun.*, vol. 34, no. 10, pp. 2605-2616, Oct. 2016.

[11] R. Saruthirathanaworakun, J. M. Peha, and L. M. Correia, "Opportunistic sharing between rotating radar and cellular," *IEEE J. Sel. Areas Commun.*, vol. 30, no. 10, pp. 1900-1910, Nov. 2012.

[12] R. Saruthirathanaworakun, J. M. Peha, and L. M. Correia, "Performance of data services in cellular networks sharing spectrum with a single rotating radar," in *Proc. IEEE WoWMoM*, Jun. 2012, pp. 1-6.

[13] A. Babaei, W. H. Tranter, and T. Bose, "A nullspace-based precoder with subspace expansion for radar/communications coexistence," in *Proc. IEEE GLOBECOM*, Dec. 2013, pp. 3487-3492.

[14] H. Deng and B. Himed, "Interference mitigation processing for spectrum-sharing between radar and wireless communication systems," *IEEE Trans. Aerosp. Electron. Syst.*, vol. 49, no. 3, pp. 1911-1919, Jul. 2013.

[15] A. Khawar, A. Abdelhadi, and T. C. Clancy, "Target detection performance of spectrum sharing MIMO radar," *IEEE Sensors J.*, vol. 15, no. 9, pp. 4928-4940, Sep. 2015.

[16] S. Biswas, K. Singh, O. Taghizadeh and T. Ratnarajah, "Coexistence of MIMO radar and FD MIMO cellular systems with QoS considerations," *IEEE Trans. Wireless Commun.*, vol. 17, no. 11, pp. 7281-7294, Nov. 2018.

[17] K. Singh *at el.*, "Transceiver design and power allocation for full-duplex MIMO communication systems with spectrum sharing radar," *IEEE Trans. Cogn. Commun. and Net.*, vol. 4, no. 3, pp. 556-566, Sep. 2018.

[18] Q. Shi *at el.*, "An iteratively weighted MMSE approach to distributed sum-utility maximization for a MIMO interfering broadcast channel," *IEEE Trans. Signal Process.*, vol. 59, no. 9, pp. 4331-4340, Sep. 2011.

[19] F. Liu, C. Masouros, A. Li, T. Ratnarajah, and J. Zhou, "MIMO radar and cellular coexistence: A power-efficient approach enabled by interference exploitation," *IEEE Trans. Signal Process.*, vol. 66, no. 14, pp. 3681-3695, 15 Jul. 2018.

[20] E. A. Gharavol, Y.-C. Liang, and K. Mouthaan, "Robust downlink beamforming in multiuser MISO cognitive radio networks with imperfect channel-state information," *IEEE Trans. Veh. Technol.*, vol. 59, no. 6, pp. 2852-2860, Jul. 2010.

[21] T. W. Ban, W. Choi, B. C. Jung, and D. K. Sung, "Multi-user diversity in a spectrum sharing system," *IEEE Trans. Wireless Commun.*, vol. 8, no. 1, pp. 102-106, Jan. 2009.

[22] H. Shajaiah, A. Khawar, A. Abdel-Hadi, and T. C. Clancy, "Resource allocation with carrier aggregation in LTE advanced cellular system sharing spectrum with S-band radar," in *Proc. IEEE DYSPAN*, Apr. 2014, pp. 34-37.

[23] M. Ghorbanzadeh, A. Abdelhadi, and C. Clancy, "A utility proportional fairness resource allocation in spectrally radar-coexistent cellular networks," in *Proc. IEEE Military Commun. Conf.*, Oct. 2014, pp. 1498-1503.

[24] L. Xu and J. Li, "Iterative generalized-likelihood ratio test for MIMO radar," *IEEE Trans. Signal Process.*, vol. 55, no. 6, pp. 2375-2385, Jun. 2007.

[25] I. Bekkerman and J. Tabrikian, "Target detection and localization using MIMO radars and sonars," *IEEE Trans. Signal Process.*, vol. 54, no. 10, pp. 3873-3883, Oct. 2006.

[26] F. Liu, C. Masouros, A. Li and T. Ratnarajah, "Robust MIMO beamforming for cellular and radar coexistence," *IEEE Wireless Commun. Lett.*, vol. 6, no. 3, pp. 374-377, Jun. 2017.
[27] S. M. Kay, *Fundamentals of statistical signal processing: Detection theory*, vol. 2, Prentice Hall, 1998.
[28] S. Boyd and L. Vandenberghe, *Convex optimization*, Cambridge, U.K.: Cambridge University Press, 2004.
[29] S. Li, R. Murch, and V. Lau, "Linear transceiver design for full-duplex multi-user MIMO system," in *Proc. IEEE ICC*, pp. 4921-4926, Jun. 2014.
[30] Y. Zhang, E. DallAnese, and G. B. Giannakis, "Distributed optimal beamformers for cognitive radios robust to channel uncertainties," *IEEE Trans. Signal Process.*, vol. 60, no. 12, pp. 6495-6508, Dec. 2012.
[31] D. P. Bertsekas, *Nonlinear Programming*, 2nd ed. Belmont, MA: Athena Scientific, 1999.
[32] A. Ben-Tal and Nemirovski, *Lectures on Modern Convex Optimization: Analysis, Algorithms, Engineering Applications*, Philadelphia, PA, USA: SIAM, 2001.
[33] D. Bertsimas, D. B. Brown, and C. Caramanis, "Theory and Applications of Robust Optimization," *SIAM Review*, vol. 53, no. 3, pp. 464-501, Aug. 2011.
[34] E. A. Gharavol and E. G. Larsson, "The sign-definiteness lemma and its applications to robust transceiver optimization for multiuser MIMO systems," *IEEE Trans. Signal Process.*, vol. 61, no. 2, pp. 238-252, Jan. 2013
[35] H. Shajaiah *at el.*, "Resource allocation with carrier aggregation in LTE advanced cellular system sharing spectrum with S-band radar," in *Proc. IEEE DYSPAN*, Apr. 2014, pp. 34-37.
[36] H. Shen, B. Li, M. Tao, and X. Wang, "MSE-based transceiver designs for the MIMO interference channel," *IEEE Trans. Wireless Commun.*, vol. 9, no. 11, pp. 3480-3489, Nov. 2010.
[37] Federal Communications Commission (FCC), *FCC proposes innovative small cell use in 3.5 GHz band*, [Online] Available: https://www.fcc.gov/document/fcc-proposes-innovative-small-cell-use-35-ghz-band, accessed, Dec. 2012.
[38] J. B. Andersen, T. S. Rappaport, and S. Yoshida, "Propagation measurements and models for wireless communications channels," *IEEE Commun. Mag.*, vol. 33, no. 1, pp. 42-49, Jan 1995.
[39] S. Sun et al., "Propagation Path Loss Models for 5G Urban Micro- and Macro-Cellular Scenarios," in *Proc. IEEE VTC Spring*, May 2016, pp. 1-6.
[40] D. Nguyen, L. Tran, P. Pirinen, and M. Latva-aho, "On the spectral efficiency of full-duplex small cell wireless systems," *IEEE Trans. Wireless Commun.*, vol. 13, no. 9, pp. 4896-4910, Sep. 2014.

Sudip Biswas (S'16, M'17) received the Ph.D. degree in Digital Communications in 2017 from the University of Edinburgh (UEDIN), UK and currently works at the Indian Institute of Information Technology Guwahati (IIITG) as an Asst. Professor in the Department of Electronics and Communications Engineering. He leads research in signal processing for wireless communications, with particular focus on 5G's long-term evolution, including transceiver design for full-duplex radios, wireless edge caching, comms-radar co-existence and large intelligent surface assisted communication. Prior to this he held the position of research associate from 2017 to 2019 at the Institute of Digital Communications in UEDIN. He also has industrial experience with Tata Consultancy Services, India (Lucknow & Kolkata), where he held the position of Asst. Systems Engineer from 2010 to 2012. He was an organizer of the IEEE International Workshop on Signal Processing Advances in Wireless Communications (SPAWC), Edinburgh, UK, 2016 and has been involved in EU FP7 projects: remote radio heads & parasitic antenna arrays (HARP) and dynamic licensed shared access (ADEL), a DST UKIERI project on wireless edge caching and an EPSRC project on NoMA.

Keshav Singh (S'12, M'16) received the degree of Master of Technology in Computer Science from Devi Ahilya Vishwavidyalaya, Indore, India, in 2006, the M.Sc. in Information & Telecommunications Technologies from Athens Information Technology, Greece, in 2009, and the Ph.D. degree in Communication Engineering from National Central University, Taiwan, in 2015. In the past, he worked as a Research Associate at the University of Edinburgh, UK. He is currently working as a Research Scientist at the University College Dublin (UCD), Ireland. His current research interests are in the areas of Green Communications, Resource Allocation, Full-Duplex Radio, Ultra-Reliable Low-Latency Communication (URLLC), Non-Orthogonal Multiple Access (NOMA), Wireless Edge Caching and Machine Learning for Communications.

Omid Taghizadeh received his the PhD degree from the Institute for Theoretical Information Technology, RWTH Aachen University in 2019 and his M.Sc. degree in Communications and Signal Processing in April 2013, from Ilmenau University of Technology, Ilmenau, Germany. Currently, he is working as a research associate at the Network Information Theory Group, Technische Universität Berlin. His research interests include full-duplex wireless systems, MIMO communications, optimization, and resource allocation in wireless networks.

Tharmalingam Ratnarajah (A'96-M'05-SM'05) is currently with the Institute for Digital Communications, the University of Edinburgh, Edinburgh, UK, as a Professor in Digital Communications and Signal Processing. He was the Head of the Institute for Institute for Digital Communications during 2016-2018. Prior to this, he held various positions at McMaster University, Hamilton, Canada, (1997-1998), Nortel Networks (1998-2002), Ottawa, Canada, University of Ottawa, Canada, (2002-2004), Queen's University of Belfast, UK, (2004-2012). His research interests include signal processing and information theoretic aspects of 5G and beyond wireless networks, full-duplex radio, mmWave communications, random matrix theory, interference alignment, statistical and array signal processing and quantum information theory. He has published over 400 papers in these areas and holds four U.S. patents. He has supervised 15 PhD students and 20 post-doctoral research fellows, and raised 11 million+ USD of research funding. He was the coordinator of the EU projects ADEL (3.7M €) in the area of licensed shared access for 5G wireless networks, HARP (4.6M €) in the area of highly distributed MIMO, as well as EU Future and Emerging Technologies projects HIATUS (3.6M €) in the area of interference alignment and CROWN (3.4M €) in the area of cognitive radio networks. Dr Ratnarajah was an associate editor for IEEE Transactions on Signal Processing (2015-2017) and technical co-chair in the 17th IEEE International workshop on Signal Processing advances in Wireless Communications, Edinburgh, UK, 2016. Dr Ratnarajah is a member of the American Mathematical Society and Information Theory Society and Fellow of Higher Education Academy (FHEA).